AIAA SciTech
13-17 January 2014, National Harbor, Maryland
52nd Aerospace Sciences Meeting

An Invariant Formulation for the Minimum Induced Drag Conditions of Non-planar Wing Systems

Demasi Luciano [*], Dipace Antonio [†], Monegato Giovanni [‡], and Cavallaro Rauno [§]

Under the hypotheses of linear potential flow and rigid wake aligned with the freestream, a configuration-invariant analytical formulation for the induced drag minimization of single-wing non-planar systems is presented. Following a variational approach, the resulting Euler-Lagrange integral equation in the unknown circulation distribution is obtained. The kernel presents a singularity of the first order and an efficient computational method, ideal for the early conceptual phases of the design, is proposed.

Munk's theorem on the normalwash and its relation with the geometry of the wing under optimal conditions is naturally obtained with the present method. Moreover, Munk's constant of proportionality, not provided in his original work, is demonstrated to be the ratio between the freestream velocity and the optimal aerodynamic efficiency. The Augmented Munk's Minimum Induced Drag Theorem is then formulated.

Additional induced drag theorems are demonstrated following the derivations of this invariant procedure.

Several non-planar wing systems are proposed and analyzed and the optimal induced drag and circulation are provided. The conjecture regarding the equality of the optimum induced drag of a quasi-closed C-wing with the induced drag of the corresponding closed system is also verified for several configurations including the boxwing.

Nomenclature

V_∞, ρ_∞	Freestream velocity and density
L	Lift
D_{ind}	Induced drag
Γ	Circulation
$\gamma(\eta)\mathrm{d}\eta$	Vortex filament
ℓ	Lifting line
η, ξ	Arc length abscissas
a	semi-length of the lifting line
u, u_v	Parameters used to represent the lifting line
y, z	Cartesian coordinates identifying a point on ℓ
v_n	Normalwash
Y	Kernel of the integral equation
λ	Lagrange multiplier
E	Aerodynamic efficiency
ε	Optimal aerodynamic efficiency ratio
α	Incidence
b_w	Semi-wingspan

[*]Associate Professor, Department of Aerospace Engineering, San Diego State University, San Diego (USA), Member AIAA, Email: ldemasi@mail.sdsu.edu

[†]PhD student, Computational Science Research Center, San Diego State University, PhD student at the Dipartimento di Ingegneria Aerospaziale, Università di Pisa. Member AIAA.

[‡]Professor, Dipartimento di Scienze Matematiche, Politecnico di Torino, Torino (Italy)

[§]PhD Candidate, Department of Aerospace Engineering, San Diego State University and Department of Structural Engineering, University of California San Diego, San Diego (USA), Member AIAA

$\mathcal{R}$	Superformula's function
μ, χ, m, p_i	Superformula's parameters
U_i	Chebyshev polynomial of the second kind of degree i
$\mathscr{L}$	Generalized Lagrange polynomial at Chebyshev nodes
$\boldsymbol{\psi}$	Even function defining a parametric representation
$\mathbf{r}$	Position vector identifying a point on ℓ
$\mathbf{i}, \mathbf{j}, \mathbf{k}$	Unit vectors of the axes of the right handed 3-D Cartesian reference
$\mathbf{v}$	Induced velocity on the lifiting line
$\boldsymbol{\tau}, \boldsymbol{n}$	Tangent and normal local unit vectors
$\mathbf{F}$	Aerodynamic force vector
$\mathbf{D}_{\text{ind}}$	Induced drag vector
$\mathbf{F}_{\perp}$	Aerodynamic force component in the direction opposite to the local normal
$(\bullet)'$	Derivative of the generic quantity $(\bullet)$

Superscripts

opt	Referred to optimal conditions
ref	Referred to the optimal conditions of the cantilever wing

Symbols

δ_{sd}	Kronecker symbol
$⨍$	Cauchy principal value

I. Introduction

INDUCED drag or drag due to lift is an important component of the total drag: it corresponds[1,2] to 30%-50% of the aircraft drag under cruise conditions. At the low speeds conditions (takeoff, landing)[3] the drag due to lift is about 80% of the total drag.

As it is argued in Reference [3], improving the aerodynamic efficiency of the takeoff portion of the flight greatly impacts the overall design with large benefits in terms of performance. This is the reason why an accurate prediction[4] (and optimization[5–7]) of the induced drag and a design of passive[8] and actively[4] controlled devices to minimize the drag due to lift interest many researchers.

The main idea behind the minimization of induced drag is to reduce, as much as possible, the gradients of the circulation.[9] This is the typical situation at the wingtips, where strong vortices are shed and the circulation (in classical cantilevered wings) goes to zero. Thus, wingtip modifications such as tip sails,[1] winglets,[10] and wing grids[11,12] achieve a significant passive reduction of the induced drag (for a fixed span).

For greater aerodynamic efficiency at different flight conditions, the induced drag can for example be reduced by control surface deflections.[13] To achieve optimal results, the calculation of these deflections should be very accurate and take into account the flexibility of the wing and consequent aeroelastic effects.[14,15]

At the early stages of the design it is useful to have a good estimate of the induced drag for a given wing configuration. A computationally efficient option is represented by panel codes.[16–20]

In the preliminary design it is also beneficial, due to the requirements of inexpensive computational methods, to evaluate the induced drag with even faster tools based on lifting line models such as the ones of References [9,21,22]. The optimal condition, when only constraints of total lift and wingspan are considered, is represented by the well known elliptical solution.[23] However, it is possible to take into account additional constraints such as the bending moment. This can be achieved as discussed in References [24–27].

Other fundamental studies on induced drag have been carried out in earlier works. Reference [28] presents the minimum induced drag conditions for V-wings and diamond ring wings. The results are obtained with an analytical method based on conformal mapping. Another significant contribution is represented by Reference [29] where analytical solutions for the minimum induced drag are again obtained with conformal transformations. In addition to the analytical results, Reference [29] reports several experimental evaluations based on the electrical analogy.

A remarkable work, surprisingly almost ignored in the open literature, is represented by Reference [30]: fundamental analytical solutions of non-planar wings (both open and closed) are used to statistically generate

a relatively simple equation for the optimal aerodynamic efficiency. Moreover, biplanes and multiplanes with different wingspans are also discussed. Reference [31] discusses several theoretical aspects of the induced drag with a rigorous mathematical approach. Particularly relevant is the qualitative plot of the optimal circulation of a joined wing configuration and a relatively simple formula derived with transformations in the complex plane (see equations 17.7 and 17.8 on page 205 and the Schwarz-Christoffel theorem on page 206). The problem of minimizing the induced drag of Joined Wings is also discussed (without showing the actual derivations) by Prandtl[9] and an approximate formula for the aerodynamic efficiency is also provided. The interest on the optimal conditions of boxwing (named Best Wing System, BWS[9]) is still quite strong nowadays. Relatively recent studies[32,33] investigate the minimum induced drag conditions under the assumption that the circulation over the joints has a butterfly-type of diagram and the load distributions over the upper/lower wing are obtained by superposing a constant and an elliptical functions. Reference [34] addresses the issue of theoretical asymptotic limit for the wings of the best wing system indefinitely distant from each other and it is observed that Prandtl's extrapolated equation (see equation 12 of Reference [9]) provides a limit of 0.16 for the ratio between the optimal induced drag referred to the classical cantilevered wing, whereas the studies conduced in References [32,33] find that limit to be 0.5. Reference [34] is based on an optimization procedure in which the aerodynamic model is represented by the vortex lattice method and finds that asymptotic limit to be 0.43[a]. It should be pointed out on this regard that the formula reported in Reference [30] for the box wing predicts an asymptotic limit of 0 (see Table 1 of Reference [30]).

The majority of these studies extensively use the very fundamental work presented by Munk[23] who introduced several important theorems to effectively identify the minimum induced drag conditions of a generic non-planar system. Particularly significant is the so called Munk's Minimum Induced Drag Theorem, which states that under optimal conditions the normalwash is proportional to the cosine of inclination of the lifting element at that point.

The present effort provides a contribution on the fundamental aspects of the induced drag minimization. With a variational approach, a configuration-invariant formulation is presented. The corresponding Euler-Lagrange equation augments Munk's Minimum Induced Drag Theorem: it is analytically obtained the value of the constant of proportionality and how it is linked to the optimal aerodynamic efficiency. Additional theorems and insights are demonstrated with the proposed invariant formulation and several non-planar test cases are presented and can provide benchmarks for the verification of accuracy and convergence characteristics of other minimization methods.

II. Contributions of the Present Work

A configuration-invariant minimization procedure is presented (see also Reference [35]). The Euler-Lagrange equation is derived with variational methods and is represented by an integral equation with a first order singular kernel. With the present method the integral equation contains only the unknown circulation and not its derivative as previously presented in other methods (see for example Reference [36] for the classical cantilevered wing and Reference [37] for a wing with curved planform).

In References [38] and [39] an alternative integral formulation was obtained. However, the singularity was of the second order and the variational method and Euler-Lagrange equation needed to be derived every time for a given wing.

On the contrary, with the proposed method, virtually any single non-planar wing can be analyzed. The derivation of the optimal condition is obtained only once and is formally invariant with respect to the wing geometry. Furthermore, the present formulation naturally leads to Munk's Minimum Induced Drag Theorem when the writing of the Euler-Lagrange equation is carried out. The constant of proportionality (originally not derived by Munk) is demonstrated to be directly related to the freestream velocity and aerodynamic efficiency under optimal conditions.

This work introduces the Minimum Induced Drag Curvature-Invariance Theorem (MIDCIT) and the Quasi-closed C-Wing Zero-gradient Optimal Circulation Theorem (QCWZOCT). In both cases, analytical proofs are provided for a generic non-planar single wing system.

A numerically efficient solution of the Euler-Lagrange equation is also discussed in detail: the aerodynamic optimal efficiency and circulation are determined in just a few seconds on a regular PC with a MATLAB code.

[a]In subsequent private conversation with the authors, E. Rizzo communicated that with a refined optimization model the numerical asymptotic limit was found to be 0.17.

Several published results are reproduced and new non-planar cases (including several winglet designs) are also presented. A detailed discussion of the C-Wing and its limit to the corresponding closed system is analyzed. It is numerically verified that the Quasi-closed C-Wing Minimum Induced Drag Conjecture (QCWMIDC) is correct: the optimal induced drag of a quasi-closed system is equal to the optimal value of the corresponding closed system. This was verified for a quasi-boxwing system. However, it should be noted that a formal proof of this property is not available in the open literature.

III. Lift, Induced Drag and Normalwash

The theory used here is based on the assumption that the wake is rigid and aligned with the freestream velocity (the x axis in Figure 1). This means that the intersection between the wake and the Trefftz plane has the exact shape of the (unstaggered[b]) lifting line ℓ. In reality, the wake is not rigid and may get distorted (wake roll up). The extent and importance of this wake deformation depends on the configuration and in the framework of preliminary design can be neglected.

Consider a symmetric and open lifting line ℓ, as shown in Figure 1. Denote by $\boldsymbol{\psi}(t) = [\psi_1(t), \psi_2(t)]^T$, $t \in [-1, 1]$ and $|\boldsymbol{\psi}'(t)| \neq 0$, an even (vectorial) function defining a parametric representation of it, and by η the corresponding arc length abscissa:

$$\eta = \eta(u) = \int_0^u \left|\boldsymbol{\psi}'(t)\right| \mathrm{d}t, \qquad \mathrm{d}\eta = \left|\boldsymbol{\psi}'(u)\right| \mathrm{d}u \tag{1}$$

where, here and in the following, $|\cdot|$ denotes the Euclidean norm. This abscissa will run from $\eta(-1) = -a$ to $\eta(1) = a$, for some positive real number a; moreover, $\eta(0) = 0$ and $\eta(-u) = -\eta(u)$. In the following, $\eta = \eta(u)$ and $\xi = \xi(u_v)$ will denote two arbitrary values of this abscissa.

Since it will be necessary to perform some Taylor expansions and to define some Cauchy principal value integrals on the curve ℓ , for simplicity it is assumed that the lifting line ℓ is sufficiently smooth. That is, it is assumed that $\psi_i(t), i = 1, 2$, are continuous functions together with their first $m \geq 2$ derivatives, in the interval $[-1, 1]$ (i.e. $\psi_i \in C^m[-1, 1]$), although this is more than what is really needed. When the arc length abscissa is used, if a point $\mathbf{r} = (y, z)^T \in \ell$, where the aerodynamic forces are calculated, is identified by its corresponding parametrization, then this will be denoted by $\mathbf{r} = \mathbf{r}(\eta) = [y(\eta), z(\eta)]^T$. When, instead, the parametric representation defined by $\boldsymbol{\psi}(t)$ is used, the same point will be denoted by $\mathbf{r} = [\psi_1(u), \psi_2(u)]^T$.

Within the assumption of lifting line theory, the aerodynamic force $\mathrm{d}\mathbf{F}$ calculated at a point of ℓ identified by the coordinate η is obtained by adding $\mathrm{d}\mathbf{F}_\perp$ (force in the direction opposite to the local normal [see Figure 1]) and $\mathrm{d}\mathbf{D}_{\mathrm{ind}}$ which is a force directed along x and parallel to the free stream velocity V_∞. $\mathrm{d}\mathbf{D}_{\mathrm{ind}}$ represents the differential of the induced drag force. If $\boldsymbol{\tau}$ indicates the unit vector tangent to the curve representing

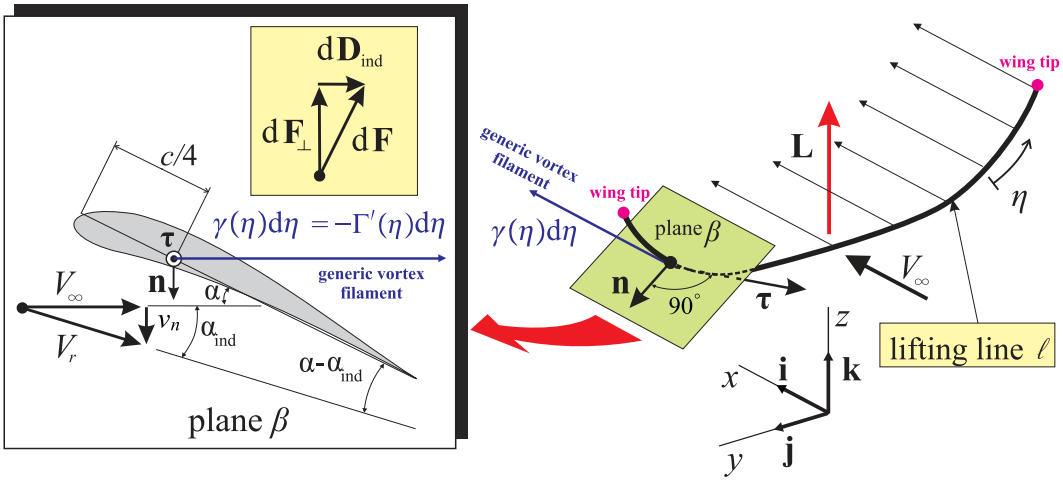

Figure 1. Aerodynamic forces and induced incidence on a profile placed in the generic point η of the curve.

[b]Munk's Stagger Theorem[23] is adopted in this work. Thus, the induced drag minimization is carried out by projecting the lifting system on a single plane perpendicular to the freestream.

the lifting line (see Figure 1) it can be inferred that

$$\begin{cases} \mathrm{d}\mathbf{F}_{\perp}(\eta) = -\rho_{\infty} V_{\infty} \Gamma(\eta)\, \mathrm{d}\eta \quad [\mathbf{i} \times \boldsymbol{\tau}(\eta)] \\ \mathrm{d}\mathbf{D}_{\mathrm{ind}}(\eta) = \rho_{\infty} \Gamma(\eta)\, \mathrm{d}\eta \quad [\mathbf{v}(\eta) \times \boldsymbol{\tau}(\eta)] \end{cases} \tag{2}$$

where $\Gamma(\eta)$ and $\mathbf{v}(\eta)$ are the values that the circulation and the induced velocity, respectively, taken at a point $\mathbf{r}(\eta) \in \ell$ identified by the coordinate η, and the symbol $\times$ denotes the classical cross (or vectorial) product. For simplicity, it is further assumed that the function $\Gamma(\eta)$ is continuous in $[-a, a]$, having also continuous derivatives of order $\leq m$ in the open interval $(-a, a)$, that is, $\Gamma \in C[-a, a] \cap C^m(-a, a)$, and that its first derivative has at most $L^p, p > 1$, integrable endpoint singularities. These assumptions are fully justified by the true physical behavior of the circulation in the case of the smooth lifting line under consideration, and it is also confirmed by the numerical testing discussed later. They allow to perform the mathematical steps needed to derive the Euler-Lagrange equation.

The circulation $\Gamma(\eta)$ is the composition of a (continuous) function $\Gamma_{\ell}(\mathbf{r})$, defined on the curve ℓ, with the parametrization $\mathbf{r} = \mathbf{r}(\eta)$. Denoting by $o(h)$ a term vanishing, as the positive quantity represented by h tends to zero, consider the following first order Taylor expansion:

$$\Gamma(\xi + \mathrm{d}\xi) = \Gamma(\xi) + \Gamma'(\xi)\mathrm{d}\xi + o(|\mathrm{d}\xi|^2), \quad -a < \xi < a \tag{3}$$

The velocity $\mathbf{v}(\eta)$ defined above is induced by the semi-infinite vortex filaments depicted in Figure 1. The generic vortex located at position ξ is indicated as $\gamma(\xi)\,\mathrm{d}\xi$. Its value can be found by applying Helmhotlz's theorem: $\gamma(\xi)\,\mathrm{d}\xi = -\Gamma'(\xi)\,\mathrm{d}\xi$.

These vortices take into account the changes of circulation Γ for a given location on the lifting line. The infinitesimal contribution $\mathrm{d}\mathbf{v}$ to the induced velocity (see Figure 2) due to the vortex $\gamma(\xi) = -\Gamma'(\xi)\mathrm{d}\xi$ and evaluated at position η (see Figure 2) is:

$$\mathrm{d}\mathbf{v}(\eta, \xi) = \frac{1}{4\pi}\, \Gamma'(\xi)\,\mathrm{d}\xi\ \ \mathbf{i} \times \frac{\mathbf{r}(\xi) - \mathbf{r}(\eta)}{|\mathbf{r}(\xi) - \mathbf{r}(\eta)|^2} \tag{4}$$

where equation 4 is an application of the Biot-Savart law. Because of the smoothness assumption that have

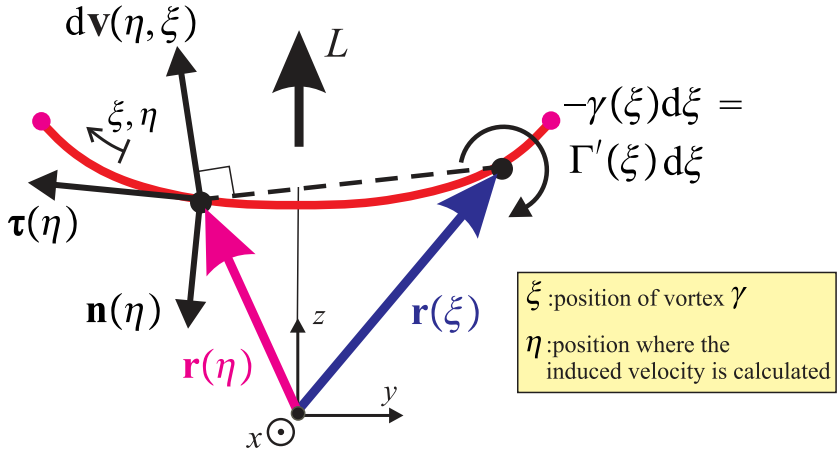

Figure 2. Infinitesimal contribution to the induced velocity calculated at location η.

been made on the curve ℓ, it is not difficult to show that

$$\frac{\mathbf{r}(\xi) - \mathbf{r}(\eta)}{|\mathbf{r}(\xi) - \mathbf{r}(\eta)|^2} = \frac{\mathbf{h}(\eta, \xi)}{\xi - \eta}, \qquad \xi \neq \eta$$

where the function $\mathbf{h}(\eta, \xi)$ and its partial derivatives of order $\leq m - 1$ are continuous with respect to both variables ($\mathbf{h} \in C^{m-1}([-a, a] \times [-a, a])$).

The expression reported on the Right Hand Side (RHS) of (4) presents a singularity when $\xi = \eta$ (i.e., the position where the induced velocity infinitesimal contribution is calculated coincides with the position

of the vortex). The singularity is of order 1; moreover, the function Γ is zero at the wing's tips. Thus, the total contribution, obtained by adding all the infinitesimal contributions due to all the vortices, is given by the following Cauchy integral:

$$\mathbf{v}(\eta) = \fint_{-a}^{a} \mathrm{d}\mathbf{v}(\eta,\xi)\,\mathrm{d}\xi = \frac{1}{4\pi} \fint_{-a}^{a} \Gamma'(\xi)\ \mathbf{i} \times \frac{\mathbf{r}(\xi) - \mathbf{r}(\eta)}{|\mathbf{r}(\xi) - \mathbf{r}(\eta)|^2}\,\mathrm{d}\xi, \qquad -a < \eta < a \tag{5}$$

where the integration limits $-a, a$ denote the curvilinear abscissa values of the wing tips. By definition (see also Figure 2), the unit normal vector is given by

$$\mathbf{n}(\eta) = \mathbf{i} \times \boldsymbol{\tau}(\eta), \tag{6}$$

where the unit vector tangent to the lifting line is easily calculated as follows:

$$\boldsymbol{\tau}(\eta) = \frac{\mathrm{d}\mathbf{r}(\eta)}{\mathrm{d}\eta} = \mathbf{r}'(\eta) \tag{7}$$

The induced drag is directed along x, whereas the lift is directed along z. Thus, the infinitesimal contributions to the lift, term $\mathrm{d}L(\eta)$, and induced drag, term $\mathrm{d}D_{\mathrm{ind}}(\eta)$, can be obtained from equation (2) as follows:

$$\begin{cases} \mathrm{d}L(\eta) = \mathrm{d}\mathbf{F}_{\perp}(\eta) \bullet \mathbf{k} = -\rho_\infty V_\infty \Gamma(\eta)\,\mathrm{d}\eta \quad [\mathbf{i} \times \boldsymbol{\tau}(\eta)] \bullet \mathbf{k} = -\rho_\infty V_\infty \Gamma(\eta)\,\mathrm{d}\eta \quad [\mathbf{k} \times \mathbf{i}] \bullet \boldsymbol{\tau}(\eta) \\ \mathrm{d}D_{\mathrm{ind}}(\eta) = \mathrm{d}\mathbf{D}_{\mathrm{ind}}(\eta) \bullet \mathbf{i} = \rho_\infty \Gamma(\eta)\,\mathrm{d}\eta \quad [\mathbf{v}(\eta) \times \boldsymbol{\tau}(\eta)] \bullet \mathbf{i} = -\rho_\infty \Gamma(\eta)\,\mathrm{d}\eta \quad [\mathbf{i} \times \boldsymbol{\tau}(\eta)] \bullet \mathbf{v}(\eta) \end{cases} \tag{8}$$

where the vector identity $(\mathbf{A} \times \mathbf{B}) \bullet \mathbf{C} = (\mathbf{C} \times \mathbf{A}) \bullet \mathbf{B}$ has been used for the first relation and the identity $(\mathbf{A} \times \mathbf{B}) \bullet \mathbf{C} = -(\mathbf{C} \times \mathbf{B}) \bullet \mathbf{A}$ has been used to elaborate the second relation. Using expression (6) and observing that $\mathbf{k} \times \mathbf{i} = \mathbf{j}$, equation (8) is rewritten as

$$\begin{cases} \mathrm{d}L(\eta) = -\rho_\infty V_\infty \Gamma(\eta)\,\mathrm{d}\eta \ \ \mathbf{j} \bullet \boldsymbol{\tau}(\eta) = -\rho_\infty V_\infty \Gamma(\eta)\,\mathrm{d}\eta\ \tau_y(\eta) \\ \mathrm{d}D_{\mathrm{ind}}(\eta) = -\rho_\infty \Gamma(\eta)\,\mathrm{d}\eta \ \ \mathbf{n}(\eta) \bullet \mathbf{v}(\eta) = -\rho_\infty \Gamma(\eta)\,\mathrm{d}\eta\ v_n(\eta) \end{cases} \tag{9}$$

The quantity $\tau_y(\eta) = \mathbf{j} \bullet \boldsymbol{\tau}(\eta)$ is the projection on the y direction of the unit vector tangent to the lifting line.

From its definition (see equation (9)) it is clear that $\mathbf{n}(\eta) \bullet \mathbf{v}(\eta) = v_n(\eta)$ represents the projection of the induced velocity on the direction perpendicular to the lifting line and the free stream velocity V_∞ (see Figure 1 for its interpretation). This is referred to as the *normalwash*. Its expression can be deduced directly from equation (5):

$$\begin{aligned} v_n(\eta) = \mathbf{n}(\eta) \bullet \mathbf{v}(\eta) &= \frac{1}{4\pi} \fint_{-a}^{a} \Gamma'(\xi)\ \ \mathbf{n}(\eta) \bullet \left[\mathbf{i} \times \frac{\mathbf{r}(\xi) - \mathbf{r}(\eta)}{|\mathbf{r}(\xi) - \mathbf{r}(\eta)|^2} \right] \mathrm{d}\xi \\ &= \frac{1}{4\pi} \fint_{-a}^{a} \Gamma'(\xi)\ \ [\mathbf{i} \times \boldsymbol{\tau}(\eta)] \bullet \left[\mathbf{i} \times \frac{\mathbf{r}(\xi) - \mathbf{r}(\eta)}{|\mathbf{r}(\xi) - \mathbf{r}(\eta)|^2} \right] \mathrm{d}\xi \end{aligned} \tag{10}$$

where equation (6) has been used. Using the vector identity $(\mathbf{A} \times \mathbf{B}) \bullet (\mathbf{C} \times \mathbf{D}) = (\mathbf{A} \bullet \mathbf{C})(\mathbf{B} \bullet \mathbf{D}) - (\mathbf{A} \bullet \mathbf{D})(\mathbf{B} \bullet \mathbf{C})$ and observing that $\boldsymbol{\tau}$ is perpendicular to $\mathbf{i}$ (see Figures 1 and 2), equation (10) is simplified as follows:

$$v_n(\eta) = \frac{1}{4\pi} \fint_{-a}^{a} \Gamma'(\xi)\ \ \boldsymbol{\tau}(\eta) \bullet \frac{\mathbf{r}(\xi) - \mathbf{r}(\eta)}{|\mathbf{r}(\xi) - \mathbf{r}(\eta)|^2}\,\mathrm{d}\xi = \frac{1}{4\pi} \fint_{-a}^{a} \Gamma'(\xi)\ Y(\eta,\xi)\,\mathrm{d}\xi \tag{11}$$

Note that the function v_n is certainly continuous in the open interval $(-a, a)$, having at most endpoint integrable singularities; that is, $v_n \in C(-a,a) \cap L^1(-a,a)$.

The quantity

$$Y(\eta,\xi) = \boldsymbol{\tau}(\eta) \bullet \frac{\mathbf{r}(\xi) - \mathbf{r}(\eta)}{|\mathbf{r}(\xi) - \mathbf{r}(\eta)|^2} = \mathbf{r}'(\eta) \bullet \frac{\mathbf{r}(\xi) - \mathbf{r}(\eta)}{|\mathbf{r}(\xi) - \mathbf{r}(\eta)|^2} = \frac{q(\eta,\xi)}{\xi - \eta} \tag{12}$$

where the function $q(\eta,\xi)$ and its partial derivatives of order $\leq m-1$ are continuous functions with respect to both variables ($q \in C^{m-1}([-a,a]\times[-a,a])$). $Y(\eta,\xi)$ is called *kernel* and presents a singularity of order 1 when $\eta=\xi$.

The normalwash v_n is directly related to the induced incidence (see Figure 1): $\alpha_{\text{ind}}(\eta) = v_n(\eta)/V_\infty$. The assumption of small angles is implied.

Integrating the contributions reported in equation (9) over the lifting line ℓ, it is possible to obtain the expressions for the lift and induced drag:

$$L = \int_\ell \mathrm{d}L = -\int_{-a}^{a} \rho_\infty V_\infty \tau_y(\eta)\ \Gamma(\eta)\ \mathrm{d}\eta \tag{13}$$

$$D_{\text{ind}} = \int_\ell \mathrm{d}D_{\text{ind}} = -\int_{-a}^{a} \rho_\infty v_n(\eta)\ \Gamma(\eta)\,\mathrm{d}\eta \tag{14}$$

It should be noted that in equation (14) the normalwash v_n (see its definition reported in (11)) involves a Cauchy integral, whereas the external integral is a standard Riemann integral. Indeed, the internal integral, as a function of η, has only endpoint logarithmic singularities.

A wing can withstand a pressure jump and the circulation Γ can be a non-null function. However, a pressure jump is not possible beyond the wing tips (see Figure 1). Thus, the circulation must be zero at those locations.

IV. Minimum Induced Drag Condition for a Single-Wing Non-planar System: the Euler-Lagrange Equation

Finding the minimum induced drag condition for a given wing span and total lift of a generic single-wing requires the minimization of a functional. This is accomplished with variational methods.[40–43] The Lagrange multiplier method is adopted to enforce the constraint of given total lift. The relative Lagrange multiplier is constant as shown in references [38] and [39].

The functional J is defined as the induced drag expression (see (14)) from which the constraint (prescribed value for the lift L_{pres}) is taken into account by using the Lagrange multiplier λ (see (14), (13), (11) and (12)):

$$J(\Gamma) = D_{\text{ind}} - \lambda(L - L_{\text{pres}}) = \int_{-a}^{a} \rho_\infty \left[-\frac{1}{4\pi} \fint_{-a}^{a} \Gamma'(\xi)\ Y(\eta,\xi)\,\mathrm{d}\xi + \lambda V_\infty \tau_y(\eta) \right] \Gamma(\eta)\,\mathrm{d}\eta + \lambda L_{\text{pres}} \tag{15}$$

Consider now a smooth arbitrary variation $\delta(\eta)$, vanishing at the endpoints $\pm a$.

A solution for the problem can be found by using the following relation (the subscript "opt" indicates the optimal condition for which J is minimized):

$$\Gamma(\cdot) = \Gamma^{\text{opt}}(\cdot) + \sigma\delta(\cdot) \qquad \sigma \in (-1,1) \tag{16}$$

where $(\cdot)$ means that the variable can be a function either of η or ξ.
Since $\Gamma(\pm a)=0$, the endpoint vanishing property of the test function $\delta(\cdot)$ implies that the optimal circulation also satisfies the homogeneous boundary conditions at the tips of the wing:

$$\Gamma^{\text{opt}}(-a) = \Gamma^{\text{opt}}(a) = 0 \tag{17}$$

To find the optimal solution, the circulation given by (16) needs to be substituted into the expression of the functional (15). Before presenting the subsequent derivations, it should be noted that in this work a non-closed path for the lifting line is assumed. Thus, this formulation is valid for any wing described by a single non-planar and non-closed lifting line (see for example the lifting line shown in Figure 1). If the wing is simulated with an open lifting line, then the circulation must be zero at the tips. This condition and the endpoint vanishing property of the test function δ are used to demonstrate (see Appendix) that the following relation holds:

$$\int_{-a}^{a} \delta(\eta) \fint_{-a}^{a} \frac{\mathrm{d}\Gamma^{\text{opt}}(\xi)}{\mathrm{d}\xi} Y(\eta,\xi)\ \mathrm{d}\xi\mathrm{d}\eta = \int_{-a}^{a} \Gamma^{\text{opt}}(\eta) \fint_{-a}^{a} \delta'(\xi)\ \ Y(\eta,\xi)\ \mathrm{d}\xi\,\mathrm{d}\eta \tag{18}$$

By means of identity (18) the functional can be written (details are omitted for brevity). To find the optimal condition, the first derivative of the functional J with respect to the parameter σ has to be calculated and equated to zero:

$$\left.\frac{\mathrm{d}J\left(\Gamma^{\mathrm{opt}}+\sigma\delta\right)}{\mathrm{d}\sigma}\right|_{\sigma=0}=\int_{-a}^{a}\rho_{\infty}\left[-2\,\frac{1}{4\pi}\int_{-a}^{a}\frac{\mathrm{d}\Gamma^{\mathrm{opt}}\left(\xi\right)}{\mathrm{d}\xi}\;Y\left(\eta,\xi\right)\;\mathrm{d}\xi\right]\;\delta\left(\eta\right)\mathrm{d}\eta+$$
$$\lambda\int_{-a}^{a}\rho_{\infty}V_{\infty}\,\tau_{y}\left(\eta\right)\;\delta\left(\eta\right)\;\mathrm{d}\eta=0 \tag{19}$$

or (see (11) for the expression of the normalwash here calculated under optimal conditions)

$$\int_{-a}^{a}\rho_{\infty}\left[-2v_{n}^{\mathrm{opt}}\left(\eta\right)+\lambda V_{\infty}\tau_{y}\left(\eta\right)\right]\;\delta\left(\eta\right)\mathrm{d}\eta=0 \tag{20}$$

The function $\delta\left(\eta\right)$ is arbitrary. This means that equation (20) implies (fundamental lemma of calculus of variations):

$$\rho_{\infty}\left[-2v_{n}^{\mathrm{opt}}\left(\eta\right)+\lambda V_{\infty}\tau_{y}\left(\eta\right)\right]=0\Rightarrow v_{n}^{\mathrm{opt}}\left(\eta\right)=\frac{1}{2}\lambda\,\tau_{y}\left(\eta\right)V_{\infty} \tag{21}$$

which is the Euler-Lagrange Equation (ELE).

The induced drag (see (14)) can then be written under optimal conditions (see (21)):

$$D_{\mathrm{ind}}^{\mathrm{opt}}=-\int_{-a}^{a}\rho_{\infty}\,v_{n}^{\mathrm{opt}}\left(\eta\right)\;\Gamma^{\mathrm{opt}}\left(\eta\right)\mathrm{d}\eta=\frac{\lambda}{2}\left[-\int_{-a}^{a}\rho_{\infty}V_{\infty}\tau_{y}\left(\eta\right)\Gamma^{\mathrm{opt}}\left(\eta\right)\;\mathrm{d}\eta\right] \tag{22}$$

The integral on the RHS represents the total lift (see (13) and consider that the lift is prescribed and known; from now on there is no need to distinguish the lift produced by a generic circulation and the prescribed value L_{pres}. Thus, in the following derivations L will indicate the prescribed lift):

$$D_{\mathrm{ind}}^{\mathrm{opt}}=\frac{\lambda}{2}L \tag{23}$$

Relationship (23) allows one to express the Lagrange multiplier λ in terms of the prescribed lift L and the unknown induced drag:

$$\lambda=\frac{2D_{\mathrm{ind}}^{\mathrm{opt}}}{L}=\frac{2}{E^{\mathrm{opt}}} \tag{24}$$

where E^{opt} is the aerodynamic efficiency under optimal conditions. Note that this representation provides a clear physical meaning for the Lagrange multiplier. By substituting expression (24) into (21) it is possible to write:

$$\alpha_{\mathrm{ind}}^{\mathrm{opt}}\left(\eta\right)=\frac{v_{n}^{\mathrm{opt}}\left(\eta\right)}{V_{\infty}}=\frac{\tau_{y}\left(\eta\right)}{E^{\mathrm{opt}}} \tag{25}$$

It is then deduced that:

The optimal induced incidence has to be proportional to the component along the y axis of the tangent-to-the-curve vector. The constant of proportionality is the inverse of the optimal aerodynamic efficiency.

V. Augmented Munk's Minimum Induced Drag Theorem

Expression (25) can be further elaborated (see (6)) for additional physical insight:

$$v_{n}^{\mathrm{opt}}\left(\eta\right)=\frac{V_{\infty}}{E^{\mathrm{opt}}}\tau_{y}\left(\eta\right)=\frac{V_{\infty}}{E^{\mathrm{opt}}}\mathbf{j}\bullet\boldsymbol{\tau}\left(\eta\right)=\frac{V_{\infty}}{E^{\mathrm{opt}}}\left[\mathbf{k}\times\mathbf{i}\right]\bullet\boldsymbol{\tau}\left(\eta\right)=\frac{V_{\infty}}{E^{\mathrm{opt}}}\left[\mathbf{i}\times\boldsymbol{\tau}\left(\eta\right)\right]\bullet\mathbf{k}=\frac{V_{\infty}}{E^{\mathrm{opt}}}\mathbf{n}\left(\eta\right)\bullet\mathbf{k} \tag{26}$$

or

$$v_{n}^{\mathrm{opt}}\left(\eta\right)=\frac{V_{\infty}}{E^{\mathrm{opt}}}\cos\left[\vartheta\left(\eta\right)\right] \tag{27}$$

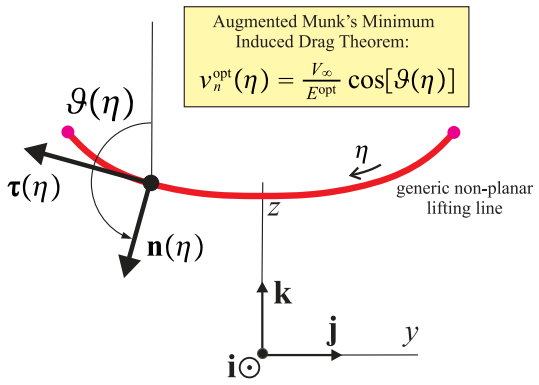

Figure 3. Augmented Munk's Minimum Induced Drag Theorem.

It is possible to observe that relationship (27) is the mathematical counterpart of Munk's Minimum Induced Drag Theorem. However, it provides *additional information not reported in the original Munk's theorem.* In fact, the original version of Munk's Minimum Induced Drag Theorem states that the normalwash has to be proportional to the cosine of ϑ (see Figure 3). With this formulation it was possible to calculate the constant of proportionality (which was not provided in the original Munk' work[c]). The "complete" theorem, defined here as *Augmented Munk's Minimum Induced Drag Theorem* (AMMIDT) is then the following[d]:

When the lifting system has been translated into a single plane (Munk's stagger theorem), the induced drag will be minimum when the component of the induced velocity normal to the lifting element at each point is proportional to the cosine of the angle of inclination of the lifting element at that point. The constant of proportionality is the ratio between the freestream velocity and the optimal aerodynamic efficiency.

A partial verification of the validity of AMMIDT beyond the formal proof presented in this work for single-wing systems, can be immediately found in Reference [39] where one can immediately deduce the same constant of proportionality for circular and elliptical annular wings.

VI. Integro-Differential Form for the Euler-Lagrange Equation

Equations (21), (25), (26) and (27) are equivalent writings of the ELE. If the ELE is satisfied, then the optimal conditions can be determined. However, these expressions are not the best practical choice when the problem needs to be numerically solved. In this case, it is convenient to rewrite the expressions in terms of the unknown circulation Γ^{opt}. This is accomplished as follows.

The optimal normalwash $v_n^{\text{opt}}(\eta)$ is explicitly calculated by means of representation (11):

$$v_n^{\text{opt}}(\eta) = \frac{1}{4\pi} \int_{-a}^{a} \frac{\mathrm{d}\Gamma^{\text{opt}}(\xi)}{\mathrm{d}\xi} \; Y(\eta, \xi) \, \mathrm{d}\xi \tag{28}$$

Then, after setting

$$\mathbf{r} = y(\eta)\mathbf{j} + z(\eta)\,\mathbf{k} \tag{29}$$

the quantity $\tau_y(\eta)$ is explicitly calculated from its definition:

$$\tau_y(\eta) = \boldsymbol{\tau}(\eta) \bullet \mathbf{j} = \frac{\mathrm{d}\mathbf{r}(\eta)}{\mathrm{d}\eta} \bullet \mathbf{j} = \frac{\mathrm{d}[\mathbf{r}(\eta) \bullet \mathbf{j}]}{\mathrm{d}\eta} = \frac{\mathrm{d}y(\eta)}{\mathrm{d}\eta} = y'(\eta) \tag{30}$$

where formula (7) has been used.

[c]The constant of proportionality can also be found by following the discussion that led to equations 20.6, 20.7, and 20.8 on page 136 of Reference [31].

[d]The wording of the original theorem has been modified for consistency of terminology of the present formulation.

Inserting expressions (30) and (28) into (25), the ELE can be written in its explicit *integro-differential form*:

$$\frac{1}{4\pi}\int_{-a}^{a}\frac{\mathrm{d}\Gamma^{\mathrm{opt}}(\xi)}{\mathrm{d}\xi}\,Y(\eta,\xi)\,\mathrm{d}\xi=\frac{V_\infty}{E^{\mathrm{opt}}}\,y'(\eta)\,,\quad -a<\eta<a \tag{31}$$

where the kernel $Y(\eta,\xi)$ is defined in (12).
The constraint of fixed total lift, defined by (13), can now be elaborated by taking advantage of identity (30):

$$L=-\int_{-a}^{a}\rho_\infty V_\infty\,\Gamma^{\mathrm{opt}}(\eta)\,\frac{\mathrm{d}y(\eta)}{\mathrm{d}\eta}\,\mathrm{d}\eta \tag{32}$$

VII. Integral Form for the Euler-Lagrange Equation

Equation (31) contains the unknown circulation differentiated with respect to the arc length abscissa. However, by applying the integration by part rule, it is possible to move the differentiation operator from the unknown circulation Γ^{opt} to the kernel.

To this end, first it is observed that the following equivalent representation of the kernel holds:

$$Y(\eta,\xi)=-\frac{\mathrm{d}}{\mathrm{d}\eta}\,\ln|\mathbf{r}(\xi)-\mathbf{r}(\eta)| \tag{33}$$

By inserting this expression into the integro-differential ELE (see equation (31)) the resulting expression is:

$$\frac{\mathrm{d}}{\mathrm{d}\eta}\left[\frac{1}{4\pi}\int_{-a}^{a}\frac{\mathrm{d}\Gamma^{\mathrm{opt}}(\xi)}{\mathrm{d}\xi}\left(-\ln|\mathbf{r}(\xi)-\mathbf{r}(\eta)|\right)\mathrm{d}\xi\right]=\frac{\mathrm{d}}{\mathrm{d}\eta}\left[\frac{V_\infty}{E^{\mathrm{opt}}}\,y(\eta)\right] \tag{34}$$

Equation (34) means that the two functions that are differentiated with respect to η must differ by a constant C:

$$\frac{1}{4\pi}\int_{-a}^{a}\frac{\mathrm{d}\Gamma^{\mathrm{opt}}(\xi)}{\mathrm{d}\xi}\left(-\ln|\mathbf{r}(\xi)-\mathbf{r}(\eta)|\right)\mathrm{d}\xi=\frac{V_\infty}{E^{\mathrm{opt}}}\,y(\eta)+C \tag{35}$$

However, for wings which are symmetric with respect to the $x-z$ plane (all the wings of practical interest have that feature) it is possible to verify that the constant C in (35) is zero. To show this property, consider the point identified by $\eta=0$ and located on the z axis. The position vector is then exactly vertical, which means that

$$y(0)=0 \tag{36}$$

Substituting condition (36) into equation (35), and assuming that $\eta=0$ identifies the point where equation (35) is evaluated, it is possible to write

$$\frac{1}{4\pi}\int_{-a}^{a}\frac{\mathrm{d}\Gamma^{\mathrm{opt}}(\xi)}{\mathrm{d}\xi}\left(-\ln|\mathbf{r}(\xi)-\mathbf{r}(0)|\right)\mathrm{d}\xi\;=C \tag{37}$$

Now focus on the integral on the LHS of equation (37).
Taking into account the symmetry of the functions $\mathbf{r}(\xi)$ and $\Gamma^{\mathrm{opt}}(\xi)$, from the Cauchy integral definition it follows:

$$\frac{1}{4\pi}\int_{-a}^{a}\frac{\mathrm{d}\Gamma^{\mathrm{opt}}(\xi)}{\mathrm{d}\xi}\left(-\ln|\mathbf{r}(\xi)-\mathbf{r}(0)|\right)\mathrm{d}\xi\;=\frac{1}{4\pi}\lim_{e\to0}\left[\int_{-a}^{-e}+\int_{e}^{a}\right]$$

$$=\frac{1}{4\pi}\lim_{e\to0}\int_{e}^{a}\left[\frac{\mathrm{d}\Gamma^{\mathrm{opt}}(\xi)}{\mathrm{d}\xi}\ln|\mathbf{r}(\xi)-\mathbf{r}(0)|-\;\frac{\mathrm{d}\Gamma^{\mathrm{opt}}(\xi)}{\mathrm{d}\xi}\ln|\mathbf{r}(\xi)-\mathbf{r}(0)|\right]\mathrm{d}\xi=0$$

That is (see (37)):

$$C=0 \tag{38}$$

The boundary condition for the optimal circulation (equation (17)) makes possible to integrate by parts the Cauchy integral reported in equation (35):

$$\begin{aligned}
&\fint_{-a}^{a} \frac{\mathrm{d}\Gamma^{\mathrm{opt}}(\xi)}{\mathrm{d}\xi} \left(-\ln|\mathbf{r}(\xi)-\mathbf{r}(\eta)|\right) \mathrm{d}\xi = \Gamma^{\mathrm{opt}}(\xi) \left(-\ln|\mathbf{r}(\xi)-\mathbf{r}(\eta)|\right)\Big|_{\xi=-a}^{\xi=a} - \\
&\fint_{-a}^{a} \Gamma^{\mathrm{opt}}(\xi) \left(-\frac{\mathrm{d}}{\mathrm{d}\xi} \ln|\mathbf{r}(\xi)-\mathbf{r}(\eta)|\right) \mathrm{d}\xi = -\fint_{-a}^{a} \Gamma^{\mathrm{opt}}(\xi)\, Y(\xi,\eta)\, \mathrm{d}\xi
\end{aligned} \tag{39}$$

where the following representation has been used (see (33)):

$$Y(\xi,\eta) = -\frac{\mathrm{d}}{\mathrm{d}\xi} \ln|\mathbf{r}(\eta)-\mathbf{r}(\xi)| \tag{40}$$

It should be noted that in the general case $Y(\xi,\eta) \neq Y(\eta,\xi)$ as can be immediately derived by direct comparison of expressions (40) and (33). Thus, the singular kernel does not present symmetry when the variables are exchanged even if the curve representing the wing has a symmetry with respect to the $x-z$ plane. Substituting (39) and (38) into equation (35), the integral form of the ELE is obtained:

$$-\frac{1}{4\pi} \fint_{-a}^{a} \Gamma^{\mathrm{opt}}(\xi)\, Y(\xi,\eta)\, \mathrm{d}\xi = \frac{V_\infty}{E^{\mathrm{opt}}}\, y(\eta), \quad -a<\eta<a \tag{41}$$

The constraint of prescribed total lift is still represented by (32).
The integral form of the ELE and the constraint (equations (41) and (32) respectively) represent a system of two equations and two unknowns: the optimal circulation $\Gamma^{\mathrm{opt}}(\xi)$ and the optimal efficiency E^{opt}. An important property of these two equations is their generality: they are valid for any non-closed non-planar single-wing system (the symmetry with respect to the $x-z$ plane is also assumed). In fact, these equations were not derived for a specific case and are configuration *invariant*. The mathematical derivation assumed the absence of corners.

Next, the following notation is adopted. Let q be a generic quantity, which can represent the circulation or another variable used in the problem of induced drag minimization. It is a function of the curvilinear coordinate η (indicated also with ξ in some cases to clearly differentiate the sending and receiving points). Then, after introducing the lifting line parametric representation $\eta=\eta(u)$ (see (1)), the composition of the functions $q(\eta)$ and $\eta=\eta(u)$ is denoted by $\widetilde{q}(u)=q(\eta(u))$.

To further simplify the above system, two quantities are introduced: the new unknown

$$\overline{\Gamma}^{\,\mathrm{opt}}(u_v) = \frac{1}{4}\frac{E^{\mathrm{opt}}\,\widetilde{\Gamma}^{\mathrm{opt}}(u_v)}{V_\infty} \tag{42}$$

and the *optimal aerodynamic efficiency ratio* ε

$$\varepsilon = \frac{L^2}{2\pi\rho_\infty V_\infty^2 b_w^2\, D_{\mathrm{ind}}^{\mathrm{opt}}} = \frac{LE^{\mathrm{opt}}}{2\pi\rho_\infty V_\infty^2 b_w^2} \tag{43}$$

where b_w is the semi-wingspan.

After introducing the changes described above, the ELE and the associated constraint take then the following form:

$$\begin{cases}
-\dfrac{1}{\pi} \displaystyle\fint_{-1}^{1} \overline{\Gamma}^{\,\mathrm{opt}}(u_v)\, \widetilde{Y}(u_v,u)\, \mathrm{d}u_v = \widetilde{y}(u), \quad -1<u<1 \\
-\dfrac{2}{\pi b_w^2} \displaystyle\int_{-1}^{1} \overline{\Gamma}^{\,\mathrm{opt}}(u)\, \widetilde{y}\,'(u)\, \mathrm{d}u = \varepsilon
\end{cases} \tag{44}$$

where

$$\widetilde{Y}(u_v,u) = \frac{\widetilde{y}\,'(u_v)\left[\widetilde{y}(u)-\widetilde{y}(u_v)\right] + \widetilde{z}\,'(u_v)\left[\widetilde{z}(u)-\widetilde{z}(u_v)\right]}{\left[\widetilde{y}(u)-\widetilde{y}(u_v)\right]^2 + \left[\widetilde{z}(u)-\widetilde{z}(u_v)\right]^2} \tag{45}$$

Remark 1 *By introducing the new unknown* $\overline{\Gamma}^{\,\mathrm{opt}}$*, the first equation in (44) does not contain the constraint and its Lagrange multiplier; thus the two equations of the system have been decoupled. Therefore, once the solution* $\overline{\Gamma}^{\,\mathrm{opt}}$ *has been determined, by inserting it into the second equation in (44), one can compute the quantity* ε*, hence* E^{opt} *and* $D_{\mathrm{ind}}^{\mathrm{opt}}$*.*

For the kernel of the first equation in (44) the representation

$$\widetilde{Y}\left(u_v, u\right) = \frac{\Theta(u_v, u)}{u_v - u} \tag{46}$$

holds, where $\Theta \in C^{m-1}([-1,1] \times [-1,1])$ satisfies the properties

$$\Theta(u,u) = \lim_{u_v \to u} \Theta(u_v, u) = 1 \tag{47}$$

and

$$\Theta(-u_v, u) = \Theta(u_v, -u) \tag{48}$$

In the following, it is assumed that the singular integral equation in (44) has a unique solution.

The uniqueness of the optimal circulation distribution has been formally demonstrated for cantilevered planar wings in Reference [36].

VIII. Physical Interpretation of the Optimal Aerodynamic Efficiency Ratio

The term *classical wing* is used in this work to indicate the cantilevered planar wing system whose lifting line is represented by a straight line. The total wingspan is indicated as $2b_w$.

Under optimal conditions the circulation distribution of this system is elliptical[23, 44] and the corresponding minimum induced drag is

$$D_{\mathrm{ind}}^{\mathrm{ref}} = \frac{L^2}{2\rho_\infty \pi V_\infty^2 b_w^2} \tag{49}$$

The *optimal aerodynamic efficiency ratio* ε previously introduced (see (43)) for a classical cantilevered wing under optimal conditions with the same wing span and lift is indicated with $\varepsilon^{\mathrm{ref}}$ and can be calculated immediately from expressions (43) and (49):

$$\varepsilon^{\mathrm{ref}} = \frac{L^2}{2\pi\rho_\infty V_\infty^2 b_w^2 \, D_{\mathrm{ind}}^{\mathrm{ref}}} = 1 \tag{50}$$

Thus, a classical cantilevered wing has optimal aerodynamic efficiency ratio equal to 1.

From equation 50 it is also deduced

$$\varepsilon^{\mathrm{ref}} = 1 = \frac{L E^{\mathrm{ref}}}{2\pi\rho_\infty V_\infty^2 b_w^2} \Rightarrow \frac{L}{2\pi\rho_\infty V_\infty^2 b_w^2} = \frac{1}{E^{\mathrm{ref}}} \tag{51}$$

where the E^{ref} is the aerodynamic efficiency for the cantilevered classical wing under optimal conditions.

Substituting (51) into (43):

$$\varepsilon = \frac{L E^{\mathrm{opt}}}{2\pi\rho_\infty V_\infty^2 b_w^2} = \frac{E^{\mathrm{opt}}}{E^{\mathrm{ref}}} \tag{52}$$

Thus, the following important property has been demonstrated:

The optimal aerodynamic efficiency ratio ε for a given wing represents the ratio between its aerodynamic efficiency and the corresponding efficiency of a reference classical cantilevered wing with the same wing span and total lift. Both efficiencies are evaluated under their respective optimal conditions.

A. Optimal Circulation and Aerodynamic Efficiency Ratio

The optimal aerodynamic efficiency ratio can also be related to the ratio between the optimal circulation, evaluated at a generic location on the wing, and the maximum value for the optimal circulation of a classical

wing (the total lift and wing span are maintained constant). To show this property, consider the *maximum value* $\Gamma_{\max}^{\text{ref}}$ for the circulation when a classical wing is under optimal conditions:

$$\Gamma_{\max}^{\text{ref}} = \frac{2L}{\rho_\infty \pi b_w V_\infty} = \frac{4V_\infty b_w}{E^{\text{ref}}} \Rightarrow E^{\text{ref}} = \frac{4V_\infty b_w}{\Gamma_{\max}^{\text{ref}}} \tag{53}$$

From the definitions of $\overline{\Gamma}^{\,\text{opt}}$ (see (42)), ε (see (52)), and $\Gamma_{\max}^{\text{ref}}$ (see (53)) the following relationship holds:

$$\overline{\Gamma}^{\,\text{opt}}(u) = \frac{\varepsilon}{\Gamma_{\max}^{\text{ref}}} b_w \widetilde{\Gamma}^{\text{opt}}(u) \tag{54}$$

from which it follows:

$$\widetilde{\Gamma}^{\text{opt}}(u) = \frac{\Gamma_{\max}^{\text{ref}}}{\varepsilon} \left(\frac{1}{b_w}\right) \overline{\Gamma}^{\,\text{opt}}(u) \tag{55}$$

B. Optimal Induced Drag and Aerodynamic Efficiency Ratio

The induced drag under optimal conditions, $D_{\text{ind}}^{\text{opt}}$, can be immediately expressed as a function of the optimal aerodynamic efficiency ratio. This is accomplished by calculating the ratio between the optimal induced drag $D_{\text{ind}}^{\text{opt}}$ for the wing under investigation and the reference optimal induced drag $D_{\text{ind}}^{\text{ref}}$ for a classical wing with the same wing span and total lift (see (52)):

$$\frac{D_{\text{ind}}^{\text{opt}}}{D_{\text{ind}}^{\text{ref}}} = \frac{E^{\text{ref}}}{E^{\text{opt}}} = \frac{1}{\varepsilon} \tag{56}$$

which implies (see (49)):

$$D_{\text{ind}}^{\text{opt}} = \frac{1}{\varepsilon} D_{\text{ind}}^{\text{Ref}} = \frac{1}{\varepsilon} \frac{L^2}{2\rho_\infty \pi V_\infty^2 b_w^2} \tag{57}$$

IX. Minimum Induced Drag Curvature-Invariance Theorem

The problem of finding the minimum induced drag for a given lift and wingspan (see system (44)) presents an important property of invariance. To discuss this property, consider a generic single-wing system symmetric with respect to the $x-z$ plane. Suppose that the minimum induced drag problem has been solved and that $\overline{\Gamma}^{\,\text{opt}}$ is the corresponding solution.

Consider now a lifting line perfectly identical to the one previously considered. Assume that this second lifting line is mirrored with respect to the first one (i.e., the two lifting lines are the symmetric image of each other with respect to the $\widetilde{y}$ axis, as Figure 4 shows). A point P on the lifting line is identified by the

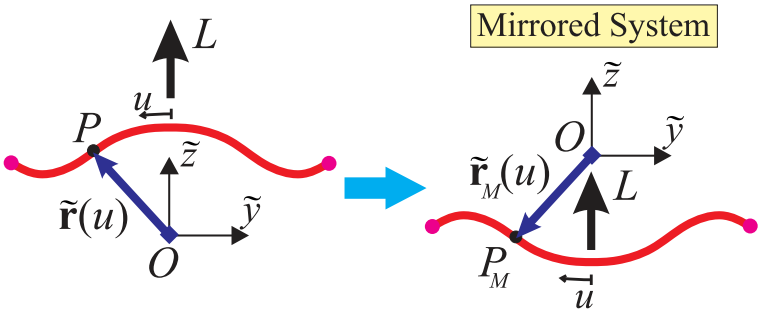

Figure 4. Identical lifting lines which are the symmetric image of each other with respect to the $\widetilde{y}$ axis.

parameter u. For the same value of the parameter, the symmetric point P_M is identified on the mirrored system. Because of the symmetry, both points P and P_M present the same y coordinate and opposite z coordinate:

$$\begin{aligned} \widetilde{y}_M(u) &= +\widetilde{y}(u) \\ \widetilde{z}_M(u) &= -\widetilde{z}(u) \end{aligned} \tag{58}$$

Similar arguments can be applied for points symmetrically located and identified by the parameter u_v. Relationships (58) and the counterpart formula written when the parameters is u_v can be used to calculate the kernel $\widetilde{Y}_M(u_v,u)$ for the mirrored system (see equation (46)):

$$\widetilde{Y}_M(u_v,u)=\frac{\widetilde{y}\,'(u_v)\left[\widetilde{y}\,(u)-\widetilde{y}\,(u_v)\right]+\widetilde{z}\,'(u_v)\left[\widetilde{z}\,(u)-\widetilde{z}\,(u_v)\right]}{\left[\widetilde{y}\,(u)-\widetilde{y}\,(u_v)\right]^2+\left[\widetilde{z}\,(u)-\widetilde{z}\,(u_v)\right]^2}\equiv\widetilde{Y}(u_v,u) \tag{59}$$

The ELE and the constraint for the mirrored system are immediately deduced from system (44) (the subscript M is now used to clearly indicate that the mirrored wing is considered):

$$\begin{cases} -\dfrac{1}{\pi}\displaystyle\int_{-1}^{1}\overline{\Gamma}_M^{\,\mathrm{opt}}(u_v)\,\widetilde{Y}(u_v,u)\,\mathrm{d}u_v=\widetilde{y}\,(u)\,, \quad -1<u<1 \\ -\dfrac{2}{\pi b_w^2}\displaystyle\int_{-1}^{1}\overline{\Gamma}_M^{\,\mathrm{opt}}(u)\,\dfrac{\mathrm{d}\widetilde{y}\,(u)}{\mathrm{d}u}\,\mathrm{d}u=\varepsilon_M \end{cases} \tag{60}$$

It is immediate to recognize that the ELE (first equation in (60)) is formally identical to the ELE of the given lifting line (see the first relation in (44)). Since it has been assumed that the ELE equation has a unique solution, this implies that

$$\overline{\Gamma}_M^{\,\mathrm{opt}}(u_v)=\overline{\Gamma}^{\,\mathrm{opt}}(u_v) \tag{61}$$

Substituting this result into the second equation in (60), the definition of ε (see (44)) is obtained. In other words, the lifting line and its mirrored counterpart have

$$\varepsilon=\varepsilon_M\Rightarrow\frac{L^2}{2\pi\rho_\infty b_w^2V_\infty^2\,D_{\mathrm{ind}}^{\mathrm{opt}}}=\frac{L_M^2}{2\pi\rho_\infty b_w^2V_\infty^2\,D_{M\,\mathrm{ind}}^{\mathrm{opt}}} \tag{62}$$

If the comparison between the lifting systems is done by maintaining the same lift (so that $L_M=L$), then from (62) it is deduced that

$$D_{\mathrm{ind}}^{\mathrm{opt}}=D_{M\,\mathrm{ind}}^{\mathrm{opt}} \tag{63}$$

which is also confirmed by the discussion presented in Reference [29] (page 23). It is then concluded that the demonstration of the the *Minimum Induced Drag Curvature-Invariance Theorem (MIDCIT)*:

Changing the sign of the curvature of the lifting line (i.e., the arc from convex is changed to concave or viceversa) does not modify the optimal induced drag and circulation distribution: the optimal solution is then invariant if the sign of the curvature is modified.

X. Quasi-Closed C-Wing Zero Gradient Optimal Circulation Theorem

When the tips of a C-wing are (symmetrically and smoothly) brought close to each other, an interesting property of the optimal circulation arises.

For notational convenience, the circulation function in the initial representation $\Gamma^{\mathrm{opt}}(\eta)$ is considered. It is recalled that this function was assumed to be uniquely defined by the ELE (41) for any value of the wing tips $\eta=\pm a$, with $\Gamma^{\mathrm{opt}}(-a)=\Gamma^{\mathrm{opt}}(a)=0$, as long as the lifting line ℓ is open. Moreover, because of the symmetry of ℓ, $\Gamma^{\mathrm{opt}}(\eta)$ is an even function, while its first derivative is odd. Thus,

$$\frac{\mathrm{d}}{\mathrm{d}\eta}\Gamma^{\mathrm{opt}}(\eta)\Big|_{\eta=-a}+\frac{\mathrm{d}}{\mathrm{d}\eta}\Gamma^{\mathrm{opt}}(\eta)\Big|_{\eta=a}=:\frac{\mathrm{d}}{\mathrm{d}\eta}\Gamma^{\mathrm{opt}}(-a)+\frac{\mathrm{d}}{\mathrm{d}\eta}\Gamma^{\mathrm{opt}}(a)=0 \tag{64}$$

for any chosen value of a (as long as the curve is open). Note that when the value of a changes, also the ELE solution changes, that is, we have $\Gamma^{\mathrm{opt}}(\eta)=\Gamma_a^{\mathrm{opt}}(\eta)$.

Now, smoothly close the (open) line ℓ symmetrically, by moving a to a value $a_0>a$, where the curve is smooth and $\eta(-a_0)=\eta(a_0)$, so that this limit curve becomes closed and smooth at any of its points. If it is assumed, as suggested by our numerical testing, that the following limit exists:

$$\lim_{a\to a_0}\frac{\mathrm{d}}{\mathrm{d}\eta}\Gamma_a^{\mathrm{opt}}(\pm a)=:\frac{\mathrm{d}}{\mathrm{d}\eta}\Gamma_{a_0}^{\mathrm{opt}}(\pm a_0)=\frac{\mathrm{d}}{\mathrm{d}\eta}\Gamma_{a_0}^{\mathrm{opt}}(a_0)$$

then, because of 64,

$$\lim_{a\to a_0}\left[\frac{\mathrm{d}}{\mathrm{d}\eta}\Gamma_a^{\mathrm{opt}}(-a)+\frac{\mathrm{d}}{\mathrm{d}\eta}\Gamma_a^{\mathrm{opt}}(a)\right]=2\frac{\mathrm{d}}{\mathrm{d}\eta}\Gamma_{a_0}^{\mathrm{opt}}(a_0)=0$$

From this, the following property finally follows:

$$\frac{\mathrm{d}}{\mathrm{d}\eta}\Gamma_{a_0}^{\mathrm{opt}}(a_0)=0$$

In other words, if the above assumption holds, and indeed this seems to be confirmed by our numerical testing, then the following *Quasi-closed C-Wing Zero-gradient Optimal Circulation Theorem (QCWZOCT)* holds:

If the two tips of a C wing are brought indefinitely close to each other, then both the optimal circulation and its first derivative tend to zero at those points.

Note that this does not mean that this property holds for the closed curve. In fact, all the results derived in this paper hold for symmetric open lifting lines. It simply means that when the line tips tend to the above common point, the values of the endpoint first derivative of Γ^{opt} tend to zero. The case of a (smooth) closed lifting line will be examined in a forthcoming paper.

XI. Minimum Induced Drag Problem: Solution Strategy

The system of equations that needs to be solved is represented by the ELE (written in its integral form) and the constraint represented by the total lift (see equation (44)). The solution strategy is then the following. *First* the curve representing the lifting line is selected. The parametrization is assumed to be known. *Second* the integral equation (first relation of equation (44)) is numerically solved (how this is accomplished will be discussed later) to obtain the unknown circulation $\overline{\Gamma}^{\,\mathrm{opt}}$. *Third*, the calculated $\overline{\Gamma}^{\,\mathrm{opt}}$ is substituted into the second relation of equation (44) and the optimal aerodynamic efficiency ratio ε is calculated. *Forth*, the specific aerodynamic efficiency is used to calculate the optimal induced drag (see equation (57)). *Fifth*, the actual circulation is calculated from equation (55).

The steps required to solve the minimization problem are graphically described in Figure 5.

Once the optimal circulation has been determined, it can be used to define the geometric parameters (the solution is not unique on this regard) of the wing (e.g, twist, chord distribution) as discussed in Reference [44].

XII. Numerical Methods

Taking into account representations (46) and (47), the ELE in equation (44) is rewritten as follows:

$$-\frac{1}{\pi}\fint_{-1}^{1}\frac{\overline{\Gamma}^{\,\mathrm{opt}}(u_v)}{u_v-u}\,\mathrm{d}u_v-\frac{1}{\pi}\int_{-1}^{1}\kappa(u_v,u)\overline{\Gamma}^{\,\mathrm{opt}}(u_v)\,\mathrm{d}u_v=\widetilde{y}\,(u),\quad -1<u<1 \tag{65}$$

where

$$\kappa(u_v,u)=\frac{\Theta(u_v,u)-\Theta(u,u)}{u_v-u}\in C^{m-2}([-1,1]\times[-1,1]),\ m\geq 2.$$

Note that

$$\kappa(u,u)=\lim_{u_v\to u}\kappa(u_v,u)=\frac{\partial\Theta(u_v,u)}{\partial u_v}|_{u_v=u}$$

and

$$\kappa(u_v,-u)=-\kappa(-u_v,u)$$

or, equivalently,

$$\kappa(-u_v,u)=-\kappa(u_v,-u).$$

and

$$\kappa(-u_v,-u)=-\kappa(u_v,u). \tag{66}$$

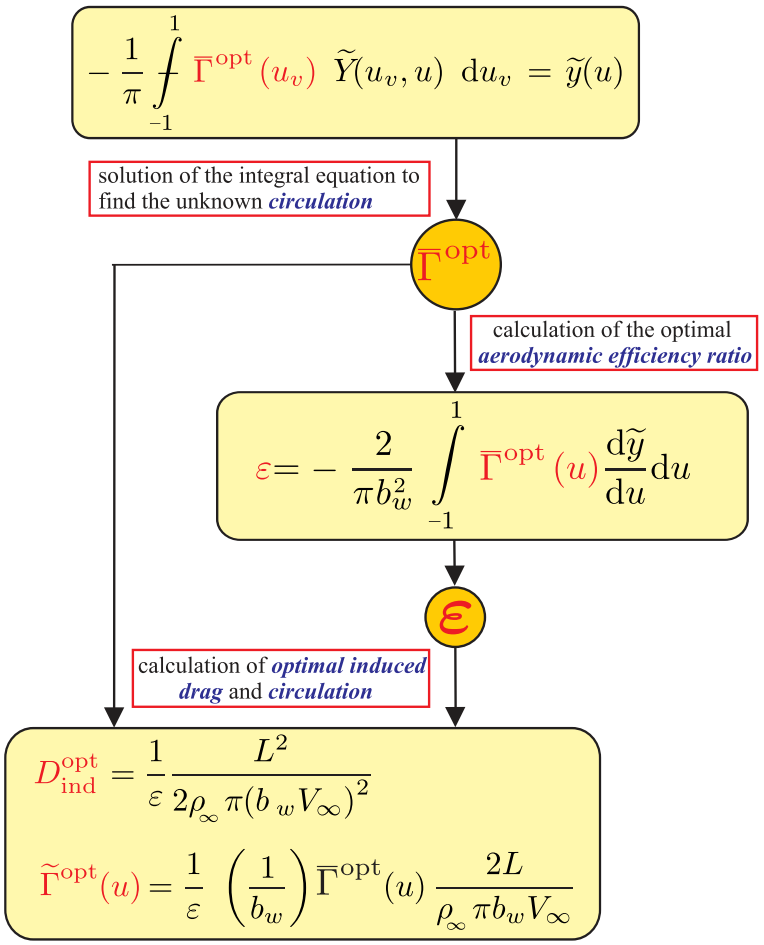

Figure 5. Minimization of induced drag for a fixed total lift and wing span: solution strategy for the case of a single-wing system.

This is a classical singular integral equation (SIE) of the first kind[45,46] that appears in many engineering problems. It has been studied by several authors, and several numerical methods have been proposed for its solution; see for example References [45–49]. In the application that is being considered in this paper, its solution $\overline{\Gamma}^{\,\mathrm{opt}}(u_v)$ is taken of the following form:

$$\overline{\Gamma}^{\,\mathrm{opt}}(u_v) = \sqrt{1-u_v^2}\,\Upsilon(u_v)$$

and is symmetric, that is, $\Upsilon(-u_v) = \Upsilon(u_v)$.

By inserting this expression in (65), the new representation is obtained:

$$-\frac{1}{\pi}\int_{-1}^{1}\sqrt{1-u_v^2}\,\frac{\Upsilon(u_v)}{u_v-u}\,\mathrm{d}u_v - \frac{1}{\pi}\int_{-1}^{1}\sqrt{1-u_v^2}\,\kappa(u_v,u)\,\Upsilon(u_v)\,\mathrm{d}u_v = \widetilde{y}\,(u), \quad -1<u<1 \tag{67}$$

i.e., in operator form,

$$(A+K)\Upsilon = \widetilde{y} \tag{68}$$

This defines a SIE of index -1.

The mapping properties of the operators A, K and $A+K$, when acting in a scale of weighted Sobolev subspaces of the Hilbert space

$$L_w^2(-1,1) = \left\{ f : \int_{-1}^{1}\sqrt{1-u^2}|f(u)|^2 du < \infty \right\}$$

have been examined in Reference [48], Section 4. In particular the authors of this paper show that when the RHS $\widetilde{y}$ and the kernel κ satisfy certain (sufficient) conditions, the SIE has a unique solution in the corresponding space. Unfortunately, all the required conditions are fulfilled except one on the kernel. This is:

$$\int_{-1}^{1} \frac{1}{\sqrt{1-u_v^2}} \kappa(u_v, u)\, \mathrm{d}u_v = 0, \qquad \forall u \in [-1, 1]$$

which is, as recognized by the same authors, very restrictive. Also results on the endpoint behavior of the solution $\Upsilon(u_v)$ are not known. These issues are by no means trivial, and will be examined in a separate paper.

Therefore, it is assumed that for the particular right hand side $\widetilde{y}\,(u)$ equation (67) has a unique solution in the space $L^2_w(-1, 1)$. Because of the symmetries of the kernel and of the known term, this solution must then be necessarily an even function. Note that the RHS function $\widetilde{y}\,(u)$ appears also in the definition of the kernel $\kappa(u_v, u)$.

To solve the above equation, among the possible numerical methods, the very simple and effective quadrature method described in Eq. (3.3) of Reference [46], and based on the classical Gaussian rule associated with the weight function $\sqrt{1-u_v^2}$ (see formula 25.4.40 of Reference [50]) is chosen. In the case of an even number of nodes, this is:

$$-\sum_{s=1}^{2n} w_s^{2n} \left[\frac{1}{u_{vs}^{2n} - u_q^{2n+1}} + \kappa(u_{vs}^{2n}, u_q^{2n+1}) \right] a_s = \widetilde{y}\,(u_q^{2n+1}), \quad q = 1 : 2n+1 \tag{69}$$

where:

$$\begin{aligned} w_s^{2n} &= \frac{1}{2n+1} \sin^2 \frac{s\pi}{2n+1}, \quad s = 1 : 2n \\ u_{vs}^{2n} &= \cos \frac{s\pi}{2n+1}, \quad s = 1 : 2n \\ u_q^{2n+1} &= \cos \frac{(2q-1)\pi}{4n+2}, \quad q = 1 : 2n+1 \end{aligned}$$

It is an over-determined set of equations, which turns out to have, however, a unique symmetric solution. By taking into account this property, which implies

$$a_{2n+1-s} = a_s, \quad s = 1 : n$$

as well as the following symmetries:

$$\begin{aligned} \widetilde{y}\,(-u) &= -\widetilde{y}\,(u) \\ \kappa\,(-u_v, u) &= -\kappa\,(u_v, -u) \\ w_s^{2n} &= w_{2n+1-s}^{2n}, \quad s = 1 : n \\ u_{vs}^{2n} &= -u_{v,2n+1-s}^{2n}, \quad s = 1 : n \\ u_q^{2n+1} &= -u_{2n+2-q}^{2n+1}, \quad q = 1 : n \end{aligned}$$

system (69) is reduced to the following one, which is of order n:

$$\sum_{s=1}^{n} w_s^{2n} \left[\frac{2u_q^{2n+1}}{[u_{vs}^{2n}]^2 - [u_q^{2n+1}]^2} + \kappa(u_{vs}^{2n}, u_q^{2n+1}) + \kappa(-u_{vs}^{2n}, u_q^{2n+1}) \right] a_s = \widetilde{y}\,(-u_q^{2n+1}), \quad q = 1 : n \tag{70}$$

Note that the equation in (69) corresponding to the collocation point $u_{n+1}^{2n+1} = 0$ (i.e., for $q = n+1$) is trivially satisfied, since both of its members are equal to zero for any given values of the coefficients a_s. Thus it must be deleted from the system.

Once this system is solved, the approximate solution is given by the following expression:

$$\Upsilon(u_v) \approx \Upsilon_{2n}(u_v) = \sum_{s=1}^{2n} a_s \mathscr{L}_s\,(u_v) \tag{71}$$

where $\{\mathscr{L}_s(u_v),\ s = 1:2n\}$ are the $(2n-1)$-degree fundamental Lagrange polynomials associated with the $2n$ zeros $\{u_{vd}^{2n}\}$ of the $2n$-degree Chebyshev polynomial of the second kind $U_{2n}(u_v)$ and defined by the interpolation conditions $\mathscr{L}_s(u_{vd}^{2n}) = \delta_{sd}$, where δ_{sd} represents the Kronecker symbol. Note that these latter imply

$$a_s = \Upsilon_{2n}(u_{vs}^{2n})$$

Furthermore, the following representation holds:

$$\mathscr{L}_s(u_v) = \frac{U_{2n}(u_v)}{(u_v - u_{vs})U'_{2n}(u_{vs})}$$

Setting $u_v = \cos(\theta_v)$, $0 \le \theta_v \le \pi$, hence $\Upsilon(u_v) = \Upsilon(\cos\theta_v)$, and recalling the representation

$$U_m(\cos\theta_v) = \frac{\sin(m+1)\theta_v}{\sin\theta_v}$$

it is not difficult to obtain the following alternative, but computationally simpler, expression for the polynomials $P_s(\cos\theta_v)$, when $\theta_v \neq \theta_{vs}$:

$$\mathscr{L}_s(\cos\theta_v) = \frac{\sin^2\theta_{vs}}{(4n+2)\sin\dfrac{\theta_v+\theta_{vs}}{2}\sin\dfrac{\theta_v-\theta_{vs}}{2}\cos(2n+1)\theta_{vs}}\frac{\sin(2n+1)\theta_v}{\sin\theta_v}$$

It is recalled that for $\theta_v = \theta_{vs}$ it is $\mathscr{L}_s(\cos(\theta_{vs}) = 1$, while if $\theta_v = 0, \pi$, the quantity $\sin(2n+1)\theta_v/\sin\theta_v$ must be replaced by its limit value, which is given by $U_{2n}(\pm 1) = 2n+1$ (see Reference [50], p.777). The following trivial identity is also recalled:

$$\frac{\sin(2n+1)\theta_v}{\sin\theta_v}\Big|_{\theta_v=\pi/2} = (-1)^n$$

Remark 2 *Since $\Upsilon_{2n}(u_v)$ is an even function, while formally it is a polynomial of degree $2n-1$, its true degree is $2n-2$.*

The optimal aerodynamic efficiency ratio ε is then computed by applying the same Gaussian rule mentioned above to the integral representation (see equation 44), that is,

$$\varepsilon = -\frac{2}{\pi}\frac{1}{b_w^2}\int_{-1}^{1}\sqrt{1-u_v^2}\,\Upsilon(u_v)\,\widetilde{y}'(u_v)\,\mathrm{d}u_v \approx -\frac{4}{b_w^2}\sum_{s=1}^{n} w_s^{2n}\,a_s\,\widetilde{y}'(u_{vs}^{2n}) \tag{72}$$

In the case of a Gaussian rule with an odd number of nodes, the proposed method takes the following form:

$$-\sum_{s=1}^{2n+1} w_s^{2n+1}\left[\frac{1}{u_{vs}^{2n+1}-u_q^{2n+2}} + \kappa(u_{vs}^{2n+1}, u_q^{2n+2})\right] a_s = \widetilde{y}\,(u_q^{2n+2}), \quad q = 1:2n+2 \tag{73}$$

where:

$$\begin{aligned} w_s^{2n+1} &= \frac{1}{2n+2}\sin^2\frac{s\pi}{2n+2}, \quad s = 1:2n+1 \\ u_{vs}^{2n+1} &= \cos\frac{s\pi}{2n+2}, \quad s = 1:2n+1 \\ u_q^{2n+2} &= \cos\frac{(2q-1)\pi}{4n+4}, \quad q = 1:2n+2 \end{aligned}$$

Also in this case there is an over-determined set of equations; however, since the solution is an even function, by taking into account this property, which implies

$$a_{2n+2-s} = a_s, \quad s = 1:n$$

as well as the symmetries of the involved quantities, as was done in the previous case, system (69) is reduced to the following one, of order $n+1$:

$$\begin{array}{l}\displaystyle\sum_{s=1}^{n} w_s^{2n+1}\left[\frac{2u_q^{2n+2}}{[u_{vs}^{2n+1}]^2-[u_q^{2n+2}]^2}+\kappa(u_{vs}^{2n+1},u_q^{2n+2})+\kappa(-u_{vs}^{2n+1},u_q^{2n+2})\right]a_s \\ +w_{n+1}^{2n+1}\left[-\frac{1}{u_q^{2n+2}}+\kappa(0,u_q^{2n+2})\right]a_{n+1}=\widetilde{y}\,(-u_q^{2n+2}),\quad q=1:n+1\end{array} \tag{74}$$

Once this system is solved, the approximate solution, an even polynomial of degree $2n$, is given by the following expression:

$$\Upsilon(u_v)\approx\Upsilon_{2n+1}(u_v)=\sum_{s=1}^{2n+1}a_s\mathscr{L}_s\,(u_v)\,,\qquad a_s=\Upsilon_{2n+1}(u_{vs}^{2n+1}) \tag{75}$$

where, for $\theta_v\neq\theta_{vs}$ it is:

$$\mathscr{L}_s(\cos\theta_v)=\frac{\sin^2(\theta_{vs}^{2n+1})}{(4n+4)\sin\dfrac{\theta_v+\theta_{vs}^{2n+1}}{2}\sin\dfrac{\theta_v-\theta_{vs}^{2n+1}}{2}\cos(2n+2)\theta_{vs}^{2n+1}}\frac{\sin(2n+2)\theta_v}{\sin\theta_v}$$

It is recalled that for when $\theta_v=0,\pi$, the quantity $\sin(2n+2)\theta_v/\sin\theta_v$ must be replaced by its limit value, which is given by $U_{2n+1}(\pm1)=\pm(2n+2)$.

Remark 3 *Unfortunately, convergence results for the above approximant $\Upsilon_m(u_v)$ to the true solution $\Upsilon(u_v)$, as $m\to\infty$, are not available. Nevertheless, in the numerical testing that has been performed, the above linear systems were non singular for all the values of n considered, and the associated approximants did show a convergent behavior. These results are very similar to those obtained by applying some alternative, but less efficient, numerical methods.*

XIII. Parameterizations of Interest and Superformula

To find the optimal circulation of a generic non-planar wing represented by the lifting line ℓ, it is necessary to evaluate the expression for the kernel (see for example equation (46)). This means that for each value of the parameter u (or u_v) the corresponding values of $\widetilde{y}$ and $\widetilde{z}$ need to be calculated.

Consider the case in which the lifting line is represented by a parabola $\widetilde{z}=\mu\widetilde{y}^{\,2}$ defined for $\widetilde{y}\in[-1,1]$. The parameter μ allows one to modify the *vertical aspect ratio* (defined as the ratio between the vertical dimension and the wingspan of the system). That is, if μ is equal to zero, then the lifting line is a straight segment (classical wing). Increasing μ to a non-zero value makes the vertical aspect ratio larger. Thus, large values of μ determine highly non-planar wings.

A parametrization of the parabola could be the following:

$$\left\{\begin{array}{rcl}\widetilde{y}\,(u) &=& -u\\ \widetilde{z}\,(u) &=& \mu u^2\end{array}\right. \tag{76}$$

where $u\in[-1,1]$.

More general parameterizations are possible. Particularly powerful is the "*superformula*"[51] which allows one to systematically obtain various natural polygons with rounded sharp edges (so that corners are not present for selected of the parameters as seen later). The parametric equation of the *superformula* is the following:

$$\left\{\begin{array}{rcl}\widetilde{y}\,(u) &=& -\mathcal{R}\,(\pi\chi u)\cdot\sin\,(\pi\chi u)\\ \widetilde{z}\,(u) &=& \mu\cdot\mathcal{R}\,(\pi\chi u)\cdot\cos\,(\pi\chi u)\end{array}\right. \tag{77}$$

where μ allows one to change the vertical aspect ratio (see previous discussion). $\mathcal{R}\,(u)$ is defined as

$$\mathcal{R}\,(\pi\chi u)=\left[\left|\cos\left(\pi\frac{m}{4}\,\chi u\right)\right|^{p_2}+\left|\sin\left(\pi\frac{m}{4}\,\chi u\right)\right|^{p_3}\right]^{-\frac{1}{p_1}} \tag{78}$$

The parameter $\chi \in [0,1]$ is provided by the user. Values of χ near zero make the represented curve close to a straight segment. Values of χ close to 1 make the curve almost a closed path.

The positive real numbers m, p_1, p_2, p_3 are also inputs. In particular, m identifies the number of rotational symmetries. If $m = 4$ and $p \equiv p_1 = p_2 = p_3 = 2$, then the superformula (77) identifies arcs of circle (when $\mu = 1$) or ellipse (when $\mu \neq 1$).

If the value of p is increased, then "quasi corners" appear. The quasi corners do not present discontinuity of the derivatives (as it would be for actual corners). The concept is shown in Figure 6.

Figure 7 shows some examples of different curves obtained from the superformula. Particularly interesting is the effect of the sign of μ: if μ is positive, then the C-wing "closes" from above. If μ is negative the reverse happens.

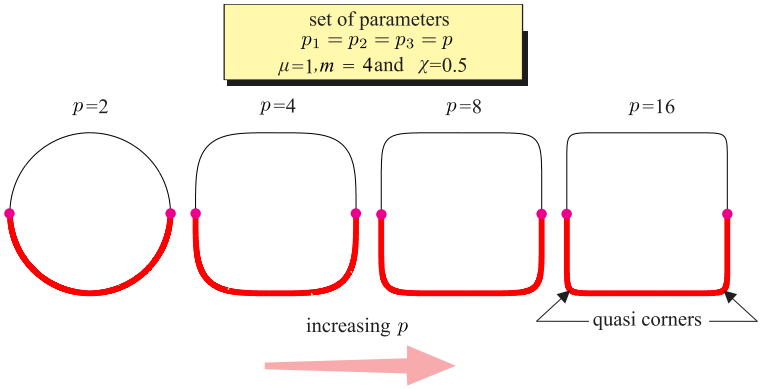

Figure 6. superformula: quasi corners obtained by increasing the parameter p.

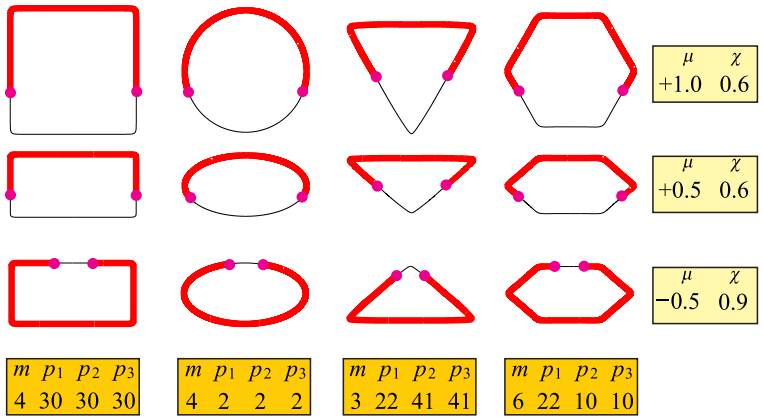

Figure 7. Superformula for different sets of the parameters

The superformula can be further exploited and more shapes can be obtained. This can be analytically shown as follows. Suppose that a given shape needs to be rotated (without violation of the symmetry with respect to z). *First* the superformula (see equation 77) is written in an auxiliary coordinate system (indicated as $\widehat{y}$ and $\widehat{z}$) and the parameter μ is set equal to 1:

$$\begin{cases} \widehat{y}(u) &= -\mathcal{R}(\pi\chi u) \cdot \sin(\pi\chi u) \\ \widehat{z}(u) &= +\mathcal{R}(\pi\chi u) \cdot \cos(\pi\chi u) \end{cases} \tag{79}$$

Second, if the figure needs to be rotated by an angle $\pi\vartheta$, then equation (79) is modified with the formal substitution $\chi u \to \chi u + \vartheta$:

$$\begin{cases} y^{\star}(u) &= -\mathcal{R}^{\star}[\pi(\chi u + \vartheta)] \cdot \sin[\pi(\chi u + \vartheta)] \\ z^{\star}(u) &= +\mathcal{R}^{\star}[\pi(\chi u + \vartheta)] \cdot \cos[\pi(\chi u + \vartheta)] \end{cases} \tag{80}$$

where $y^\star$, $z^\star$, and $\mathcal{R}^\star$ are the new quantities obtained after the above mentioned formal substitution is implemented.

Third, the actual dimensionless coordinates $\widetilde{y}$ and $\widetilde{z}$ are obtained from (80) by multiplication of the rotation matrix. The factor μ is introduced at this stage to change the wing vertical aspect ratio:

$$\begin{bmatrix} \widetilde{y}\,(u) \\ \widetilde{z}\,(u) \end{bmatrix} = \begin{bmatrix} \cos(\pi\vartheta) & \sin(\pi\vartheta) \\ -\mu\sin(\pi\vartheta) & \mu\cos(\pi\vartheta) \end{bmatrix} \begin{bmatrix} y^\star\,(u) \\ z^\star\,(u) \end{bmatrix} \tag{81}$$

The superformula corresponding to the rotated shape is then

$$\begin{cases} \widetilde{y}\,(u) = \mathcal{R}^\star\left[\pi\left(\chi u+\vartheta\right)\right]\cdot\left[-\sin\left[\pi\left(\chi u+\vartheta\right)\right]\cdot\cos(\pi\vartheta)+\cos\left[\pi\left(\chi u+\vartheta\right)\right]\cdot\sin(\pi\vartheta)\right] \\ \widetilde{z}\,(u) = \mu\mathcal{R}^\star\left[\pi\left(\chi u+\vartheta\right)\right]\cdot\left[+\sin\left[\pi\left(\chi u+\vartheta\right)\right]\cdot\sin(\pi\vartheta)+\cos\left[\pi\left(\chi u+\vartheta\right)\right]\cdot\cos(\pi\vartheta)\right] \end{cases} \tag{82}$$

The concept is explained in Figure 8.

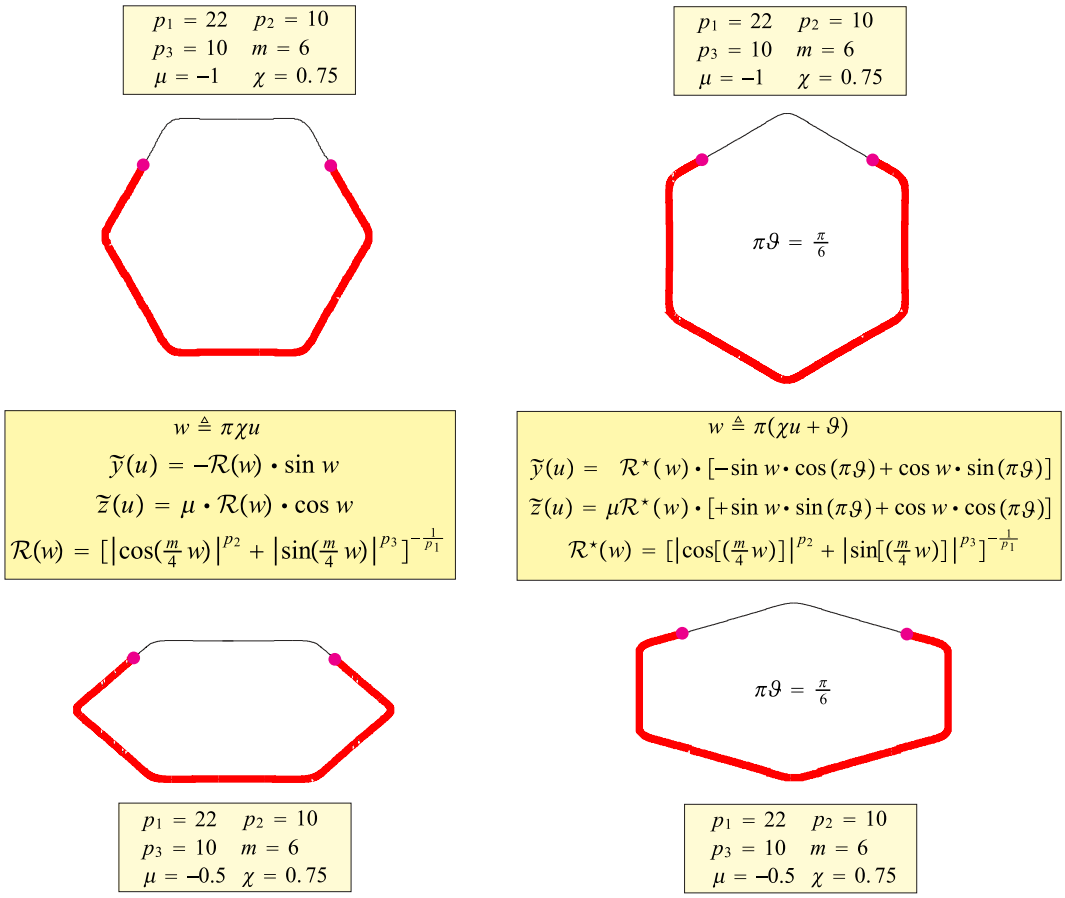

Figure 8. Example of modification of the Superformula.

As previously anticipated, not all values of the parameters provide corner-free curves. It should be noted that the mathematical derivations and demonstrations of this work are valid only for curves that do not present any corner. Thus, the selection of the superformula's parameters needs to be done with care. Unless otherwise specified, the superformula used in the different cases is reported in (77) and (78).

The invariant procedure proposed in this work can also be used if the geometry is described by a smooth piecewise function (with no corners). This means, for example, that (smooth) cubic splines could be effectively employed to investigate wings of interest for the designer.

XIV. Results

A. Numerical Study: Convergence Test

The numerical solution is carried out by adopting the procedure shown in Figure 5. The crucial part is the solution of the integral equation. The method is discussed in section XII. Figure 9 shows a convergence study for a C-wing which is obtained from the superformula (equations (77) and (78)) by setting the parameters shown in the figure. It can be observed that when parameter n (see equation (71) and Figure 9) is larger than 50 the solution practically does not change and a convergence is reached. Moreover, the convergence of the optimal aerodynamic efficiency ratio ε is even faster and with $n = 40$ the correct value is reached.

In the authors' experience the wing system of Figure 9 is one of the most numerically challenging cases. Nevertheless, the performance of the numerical method is excellent. In other cases a far smaller number of terms is sufficient to achieve the desired accuracy.

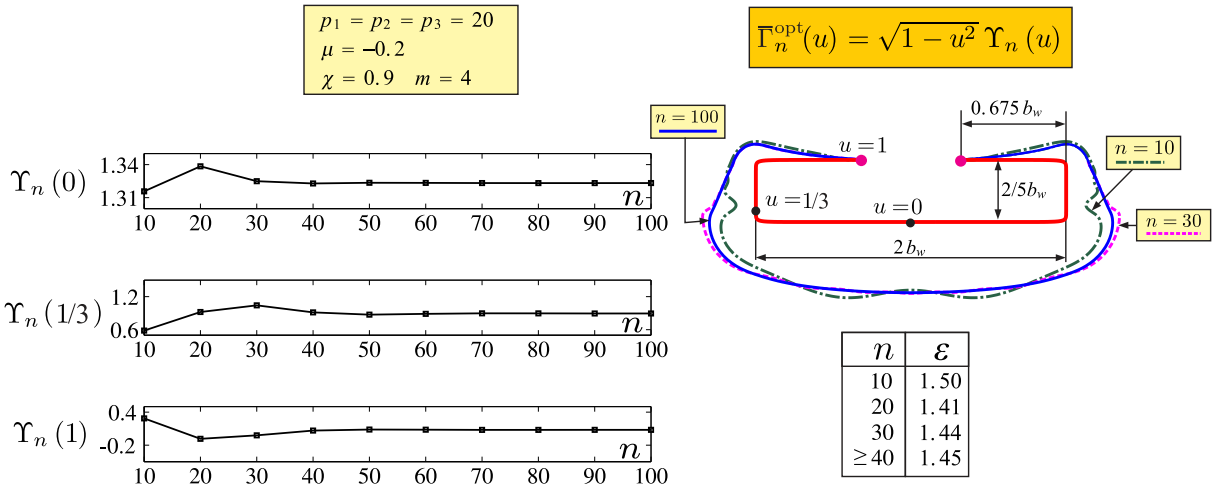

Figure 9. Study of the convergence of the numerical method

B. Validation

The present invariant procedure for the induced drag minimization correctly predicts the well known result[44] about the classical wing loaded with elliptical distribution. The analytical derivations proving this fact are omitted for brevity.

Other validations are performed by comparing the aerodynamic specific efficiency with known[39] values relative to lifting lines represented by circular arcs. The correlation is excellent (see Figure 10). Other validations will be presented later when the C-wings will be discussed.

In all the results the prescribed lift (not relevant as far as the specific aerodynamic efficiency is concerned) is modified case by case so that the graphical plots of the optimal circulation are the clearest possible.

C. Effects of the Vertical Aspect Ratio

To investigate the effect of the vertical aspect ratio, a wing whose lifting line is a parabola is considered. That is, the lifting line has equation $\widetilde{z} = \mu \widetilde{y}^2$. Figure 11 shows that increasing μ (and so the vertical aspect ratio) reduces the optimal induced drag $D_{\text{ind}}^{\text{opt}}$ with respect to the reference value $D_{\text{ind}}^{\text{ref}}$ represented by the optimal induced drag of an elliptically loaded cantilevered wing. Figure 11 also shows the optimal circulation distributions for $\mu = 0$ (case of classical wing), $\mu = 0.25$, and $\mu = 0.5$. A simplified formula for the ratio $D_{\text{ind}}^{\text{opt}}/D_{\text{ind}}^{\text{ref}}$ is also provided in Figure 11. It can be observed that increasing the vertical aspect ratio is highly beneficial as far as the induced drag is concerned. It has been numerically verified that very large vertical aspect ratios produce practically induced-drag-free systems. This is in agreement with the tables reported in Reference [30] and with the discussion reported in section 20, page 135 of Reference [31].

Another interesting qualitative aspect is that the gradients of the optimal circulation decrease in magnitude when the vertical aspect ratio is increased (see Figure 12). This is consistent with the observation

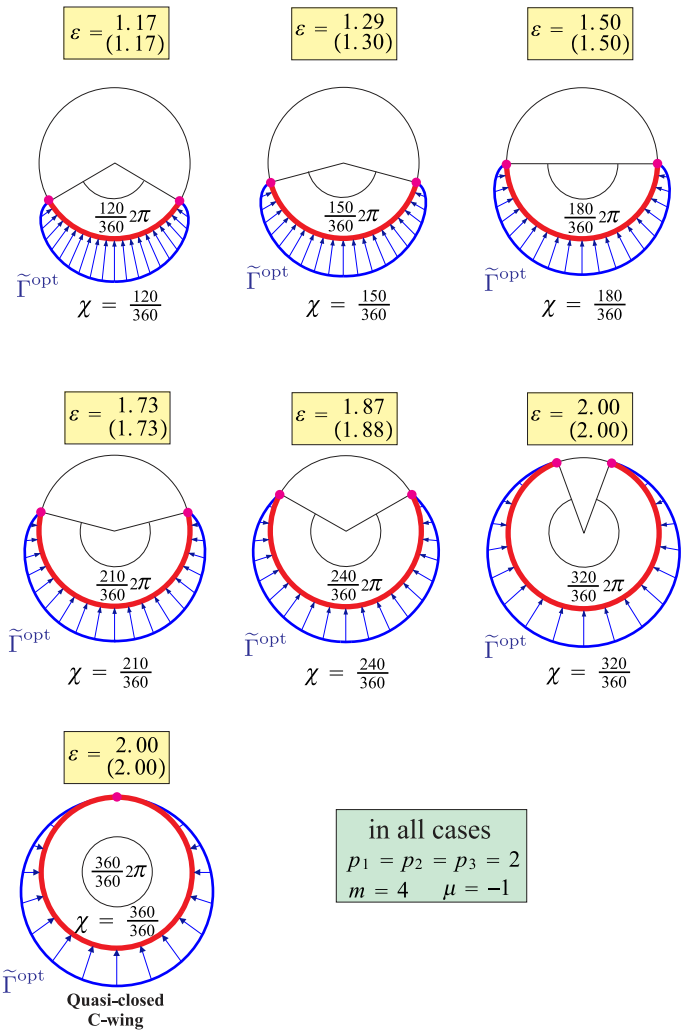

Figure 10. Optimal conditions of lifting arcs: validation. In parenthesis the results obtained from Reference [39] are reported.

that high vertical aspect ratio corresponds to very low levels of induced drag, quantity that is known to be directly linked to the gradients of the circulation.

D. Effects of the Winglets on the Induced Drag

It is well known that the adoption of winglets substantially reduces the induced drag. Different design options are possible. A few of these options are presented in Figure 13. It is possible to observe that the vertical winglets provide the best specific aerodynamic efficiency. However, the lowest induced drag is obtained by having an obtuse angle (which determines a higher wing span, see Figure 13 c)).

E. Effects of the Wing Curvature on the Optimal Induced Drag

As previously discussed in section XIII, changing the parameters of the superformula dramatically changes the shape of the lifting line (see Figure 6). This also affects the induced drag, as demonstrated in Figure 14. In particular, if the C-wing becomes increasingly similar to a portion of rectangle (Figure 14) then the optimal induced drag is substantially reduced.

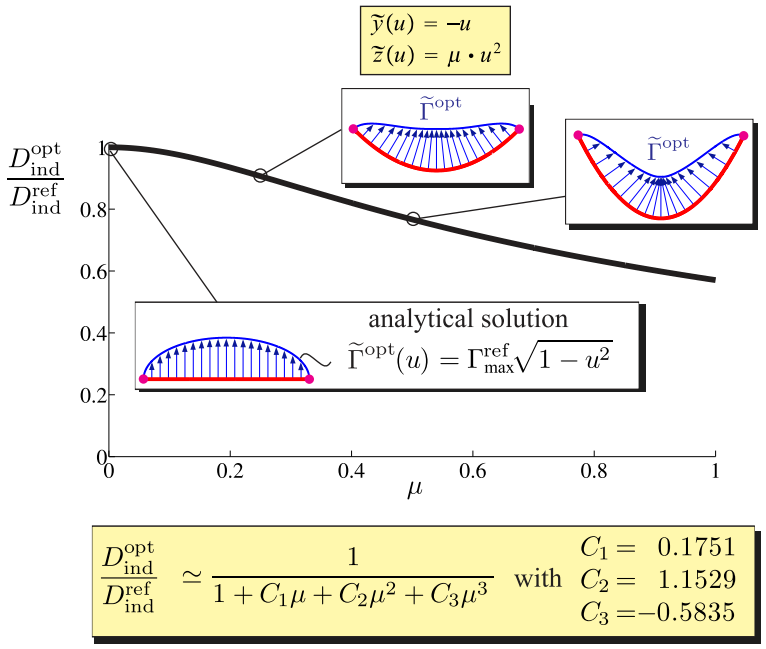

Figure 11. Optimal induced drag of a parabolical wing for increasing vertical aspect ratio.

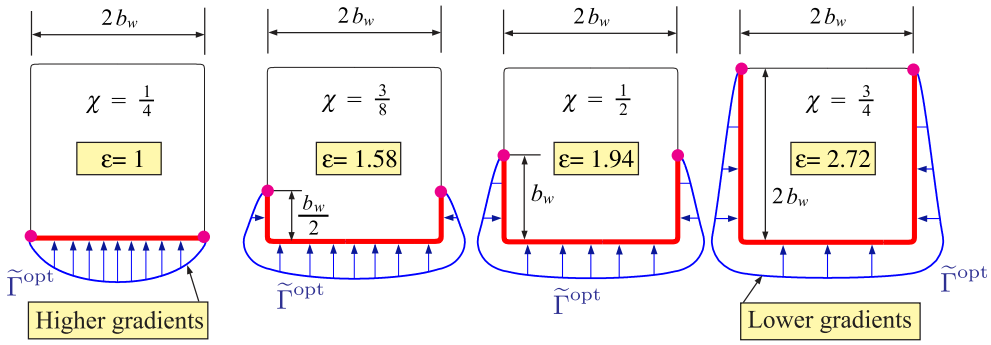

Figure 12. Variation of the optimal circulation and specific aerodynamic efficiency with increasing vertical aspect ratio. In all these cases it is $p_1 = p_2 = p_3 = 40$ and $m = 4$.

F. Quasi-Closed C-Wing Minimum Induced Drag Conjecture (QCWMIDC)

It is of a relevant engineering interest to investigate what happens when the C-wing is modified until it becomes a quasi-closed system. Figure 15 presents the results. It can be observed a reduction of the gradients of the optimal circulation (fact earlier noted) when the system is almost a closed system. Moreover, the optimal induced drag is reduced. Reference [39] analytically demonstrated that the optimal distribution is not unique and adding a constant circulation does not change the optimal induced drag. However, the demonstration was limited to elliptical annular wings. This concept is also included by Kroo in Reference [10], where a discussion on *closed* systems is presented. In particular, it is possible to read (page 17):

...the optimal load distribution is not unique. One may superimpose a vortex loop with constant circulation on any of these wing geometries. This changes the local loading, but because the circulation is constant, the wake (and hence the lift and drag) is unchanged.

Moreover, Kroo links on page 18 this fact to the C-wing concept:

...We can, however, add a fixed circulation to the [closed] system so that the lower wing carries the entire lift and the upper wing carries none. The lift and vortex drag are unchanged. This is the reason that the C-wing geometry in figure 2 so closely approximates the drag of the boxplane: we simply adjust the constant circulation increment so that the inner part of the upper wing is not needed.

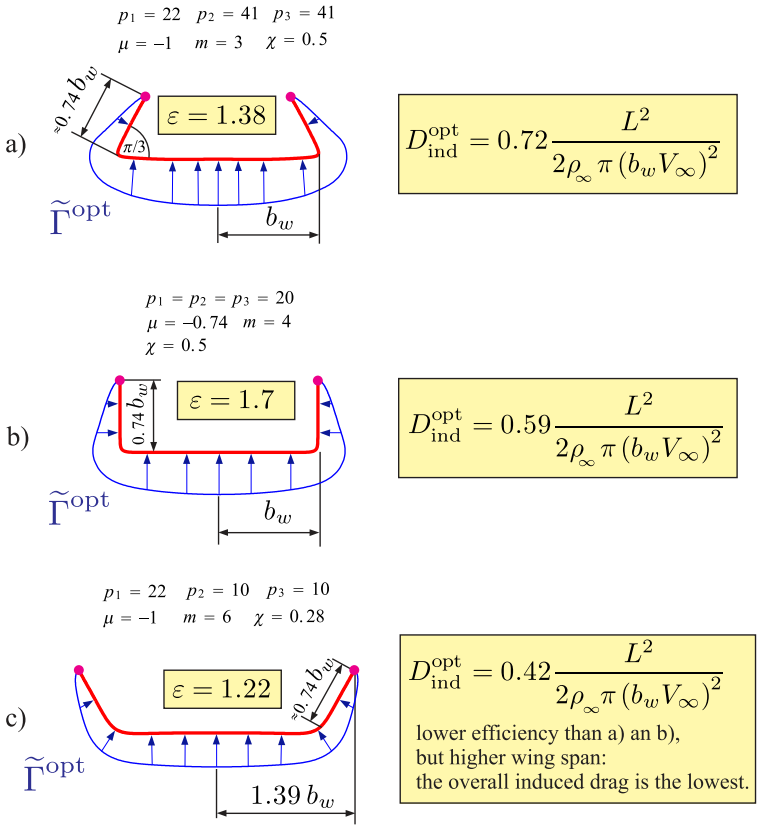

Figure 13. Optimal conditions for different types of winglets.

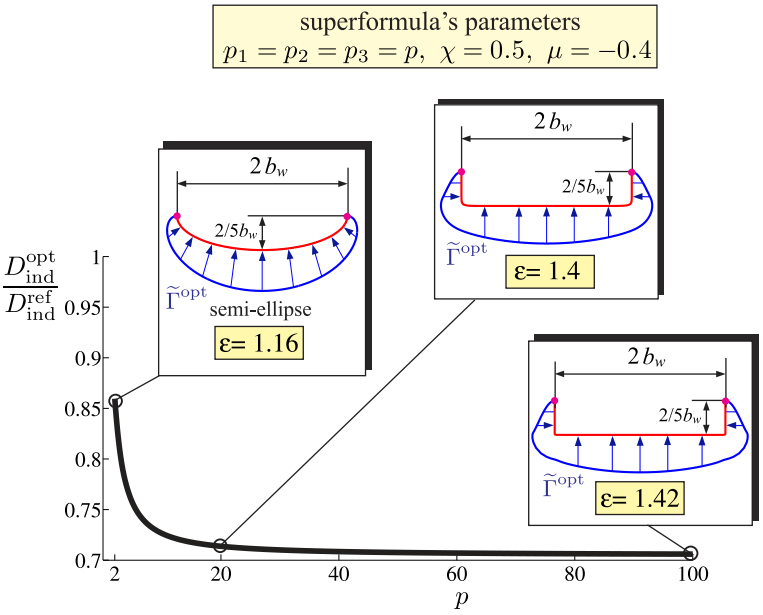

Figure 14. The parameter p is associated with the curvature of the wing. For $p = 2$, the C-wing is a semi-ellipse, while for $p \to \infty$ the C-wing presents quasi-corners.

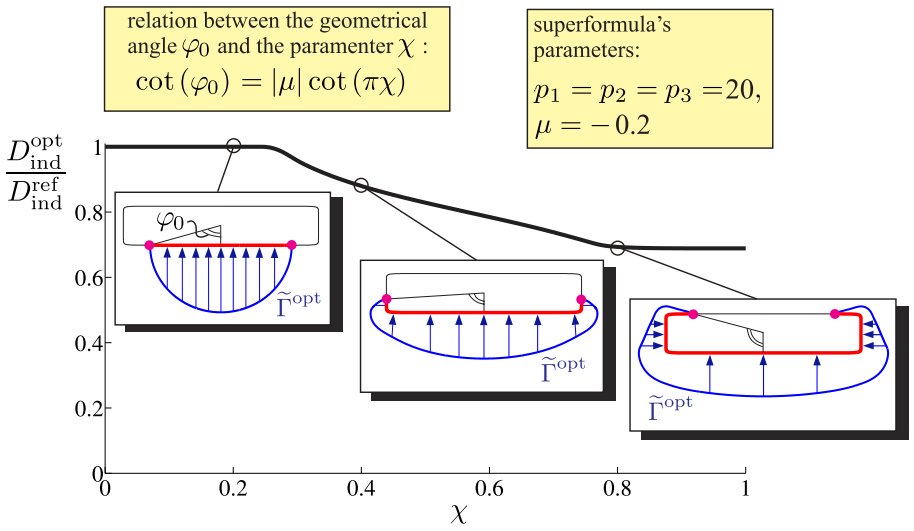

Figure 15. Quasi-closed C-wing system.

These concepts are also graphically presented in Figure 24 of Reference [39]. However, the fact that a *quasi-closed C-wing* presents the same optimal induced drag has *not* been formally demonstrated in the literature. What References [10] and [39] report is named here *Quasi-closed C-Wing Minimum Induced Drag Conjecture (QCWMIDC)*.

QCWMIDC is verified in Figure 10, where the quasi-closed circular arc presents the same optimal induced drag (and efficiency) of the corresponding circular wing.[29,39] Another qualitative proof of QCWMIDC can be derived by taking the boxwing introduced in Reference [10] and presenting a height-to-wingspan ratio equal to 0.2. As can be seen from Figure 16, the conjecture is verified. Moreover, the present invariant

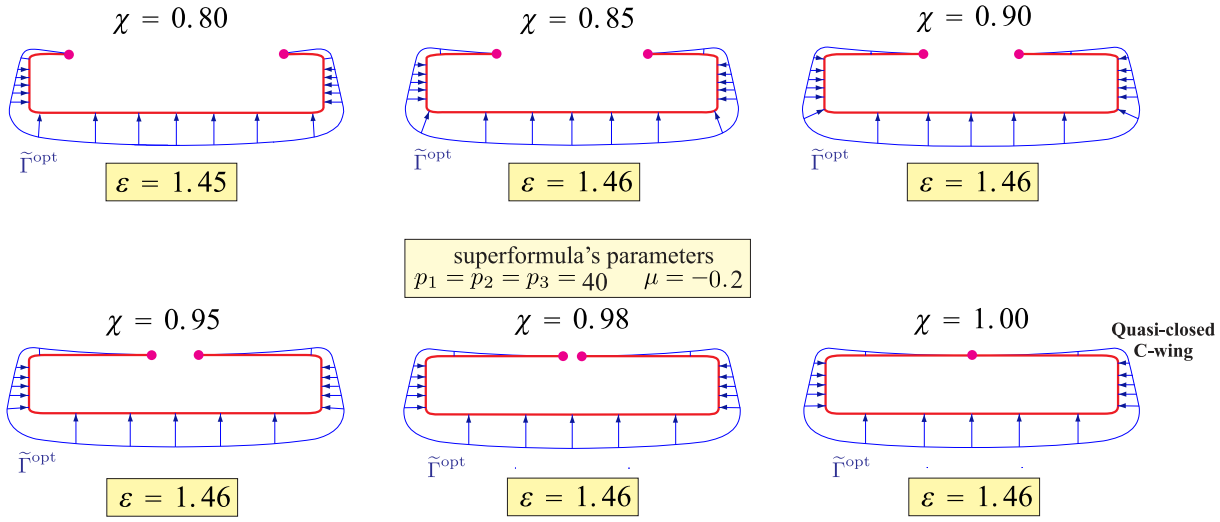

Figure 16. Verification of the Quasi-Closed C-Wing Minimum Induced Drag Conjecture.

minimization procedure exactly reproduces the value of the specific aerodynamic efficiency of 1.46 as can be seen on Figure 2 of Reference [10]. It should be noted that all the wings analyzed in Figure 16 were obtained by setting $\mu = -0.2$. If all the other parameters are kept the same but it is set $\mu = 0.2$, then a mirrored system is obtained and the optimal induced drag and aerodynamic specific efficiency do not change. In other words, it has been numerically verified the Minimum induced Drag Curvature-Invariance Theorem earlier demonstrated.

QCWMIDC is also verified for elliptical annular wings, for which there is analytical closed-form solution

of the specific aerodynamic efficiency.[39] The details are omitted for brevity.

G. Minimum Induced Drag Conditions for Wings of Various Shapes

The present invariant induced drag minimization procedure is now adopted to study various configurations.

1. *Optimal Distributions and Specific Aerodynamic Efficiencies for V-Shaped Wings*

The optimal circulation and specific aerodynamic efficiency of various cases are reported in Figure 17. The beneficial effects of vertical aspect ratio and winglets are confirmed.

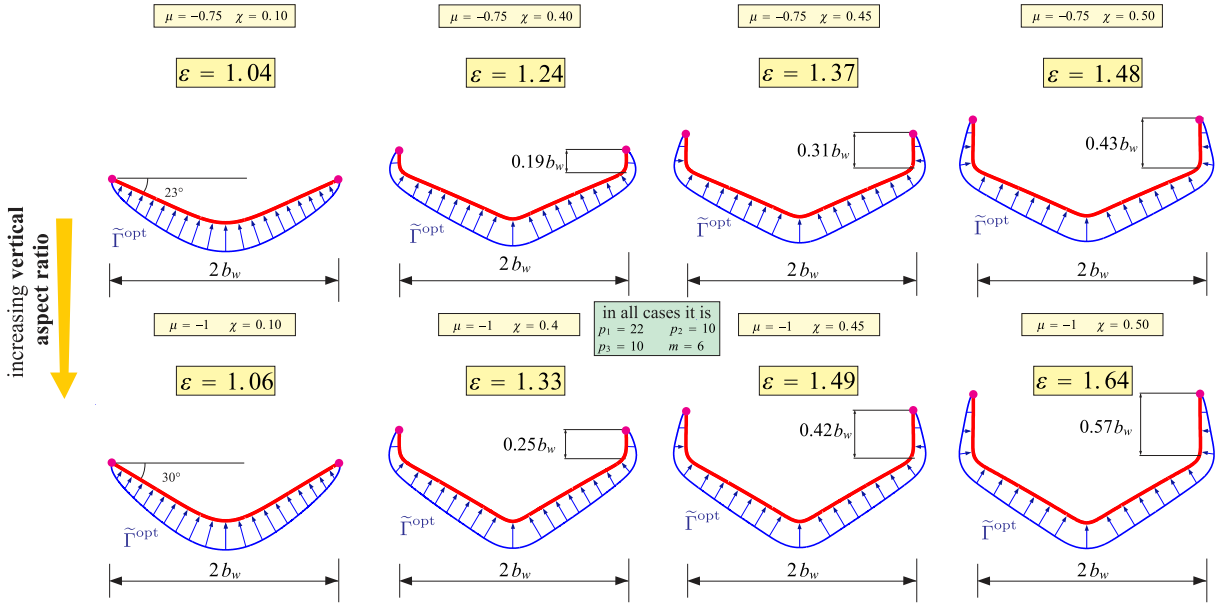

Figure 17. Optimal conditions for various V-shaped wings and effects of winglets. The superformula used to generate these cases is reported in equation 82

2. *Optimal Distributions and Specific Aerodynamic Efficiencies for Highly Non-planar Wings*

Figures 18, 19, and 20 show the optimal circulation distribution and specific aerodynamic efficiencies for various configurations. It is confirmed that highly non-planar wings present great beneficial in the induced drag reduction. It can also be observed that the Quasi-Closed C-Wing Zero Gradient Optimal Circulation Theorem is satisfied. This confirms the analytical demonstration earlier presented (see the discussion presented in section X).

XV. Conclusions

Under the hypotheses of linear potential flow and rigid wake aligned with the freestream, an invariant formulation for the induced drag minimization of a generic non-planar single-wing system has been presented for the first time. The Euler-Lagrange equation is obtained with a variational method. It is an integral equation which contains only the unknown circulation and not its derivatives. The kernel presents a first order singularity.

Munk's Minimum Induced Drag Theorem is naturally deduced in the derivation of the optimal conditions and the constant of proportionality, not explicitly reported by Munk, is determined in this work. The original theorem presented by Munk is then reformulated as the *Augmented Munk's Minimum Induced Drag Theorem* (AMMIDT):

When the lifting system has been translated into a single plane (Munk's stagger theorem), the induced drag will be minimum when the component of the induced velocity normal to the lifting element at each point is

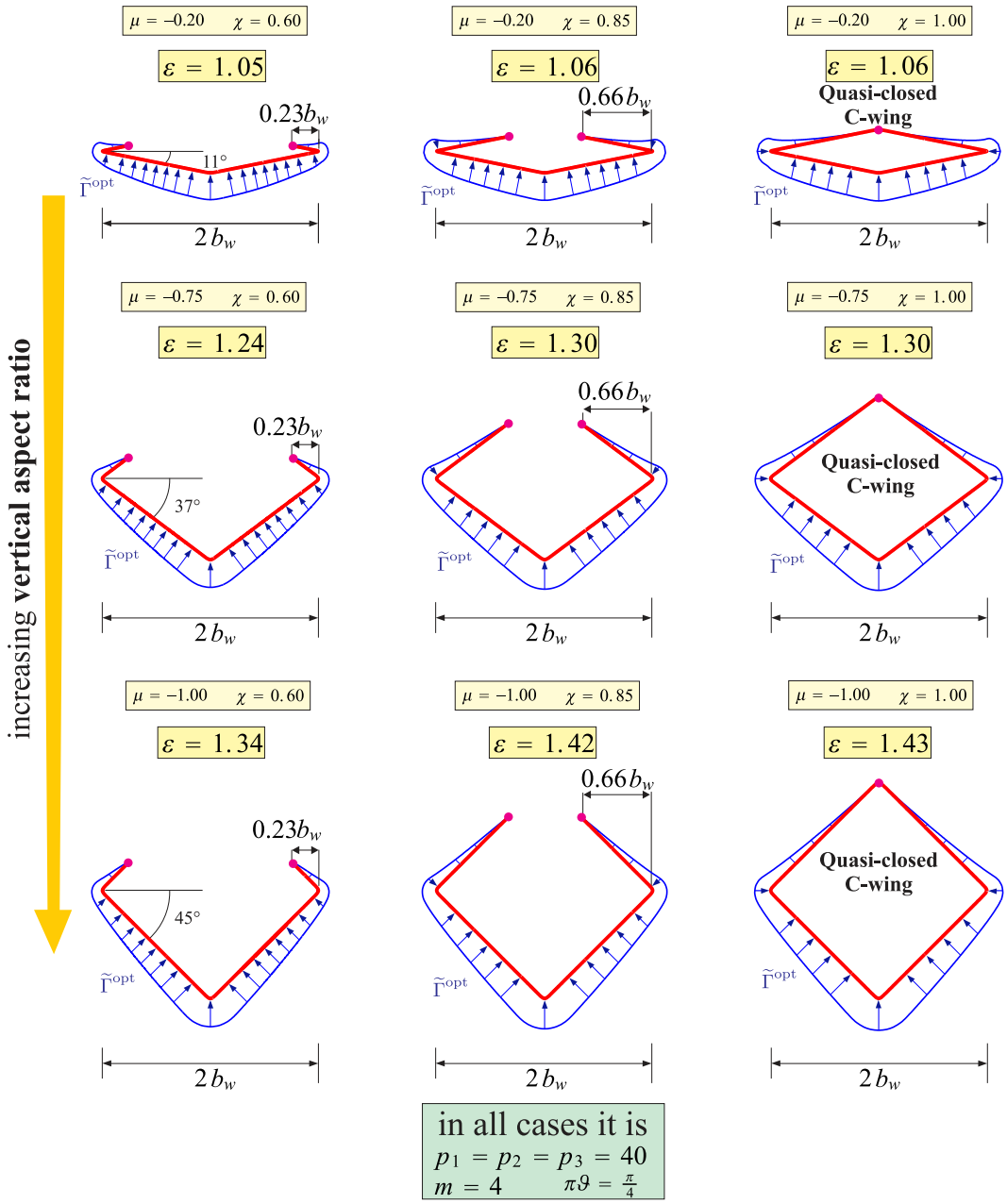

Figure 18. Optimal conditions for various highly non-planar wings. The superformula used to generate these cases is reported in equation 82

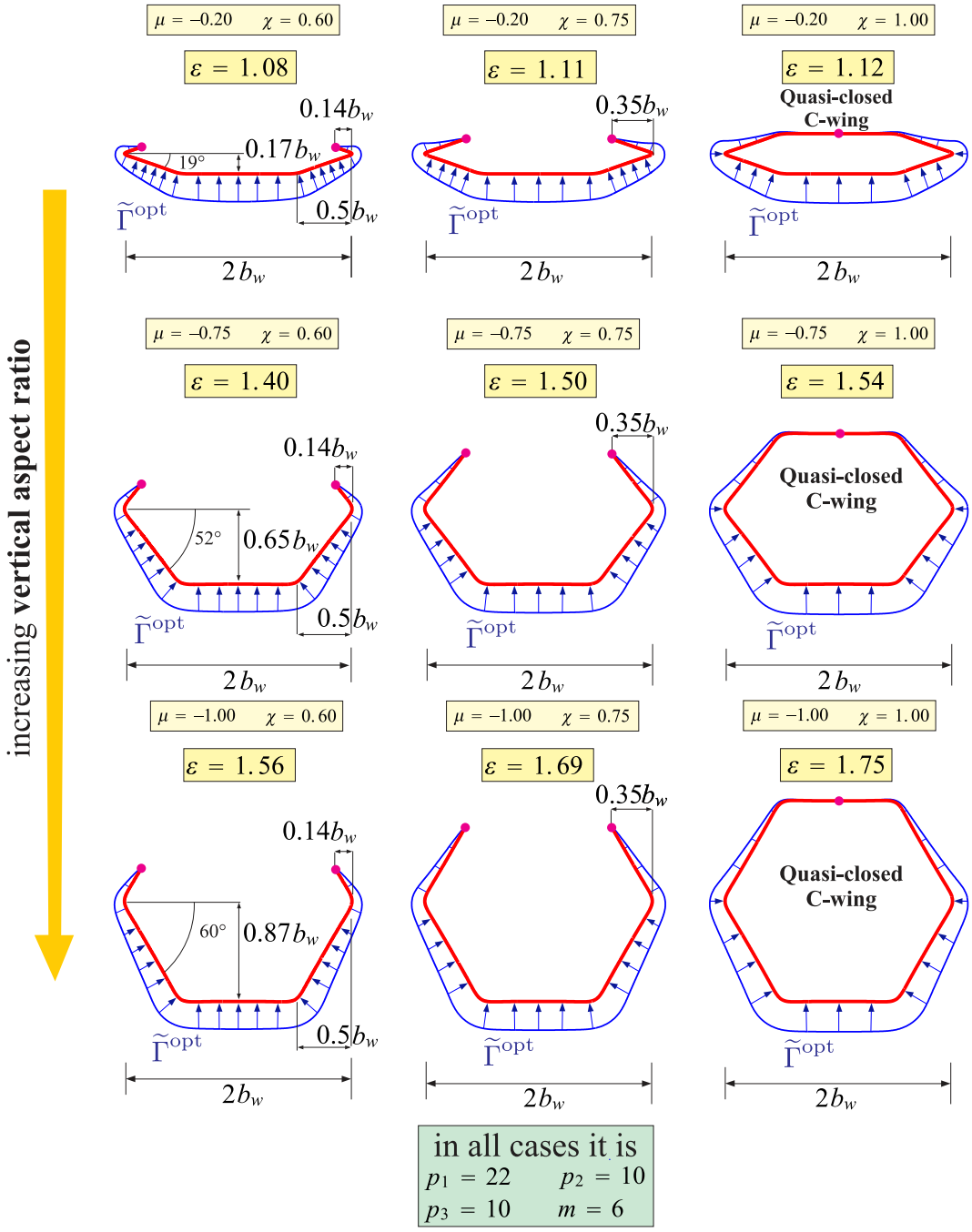

Figure 19. Optimal conditions for various highly non-planar wings. The superformula used to generate these cases is reported in equation 77

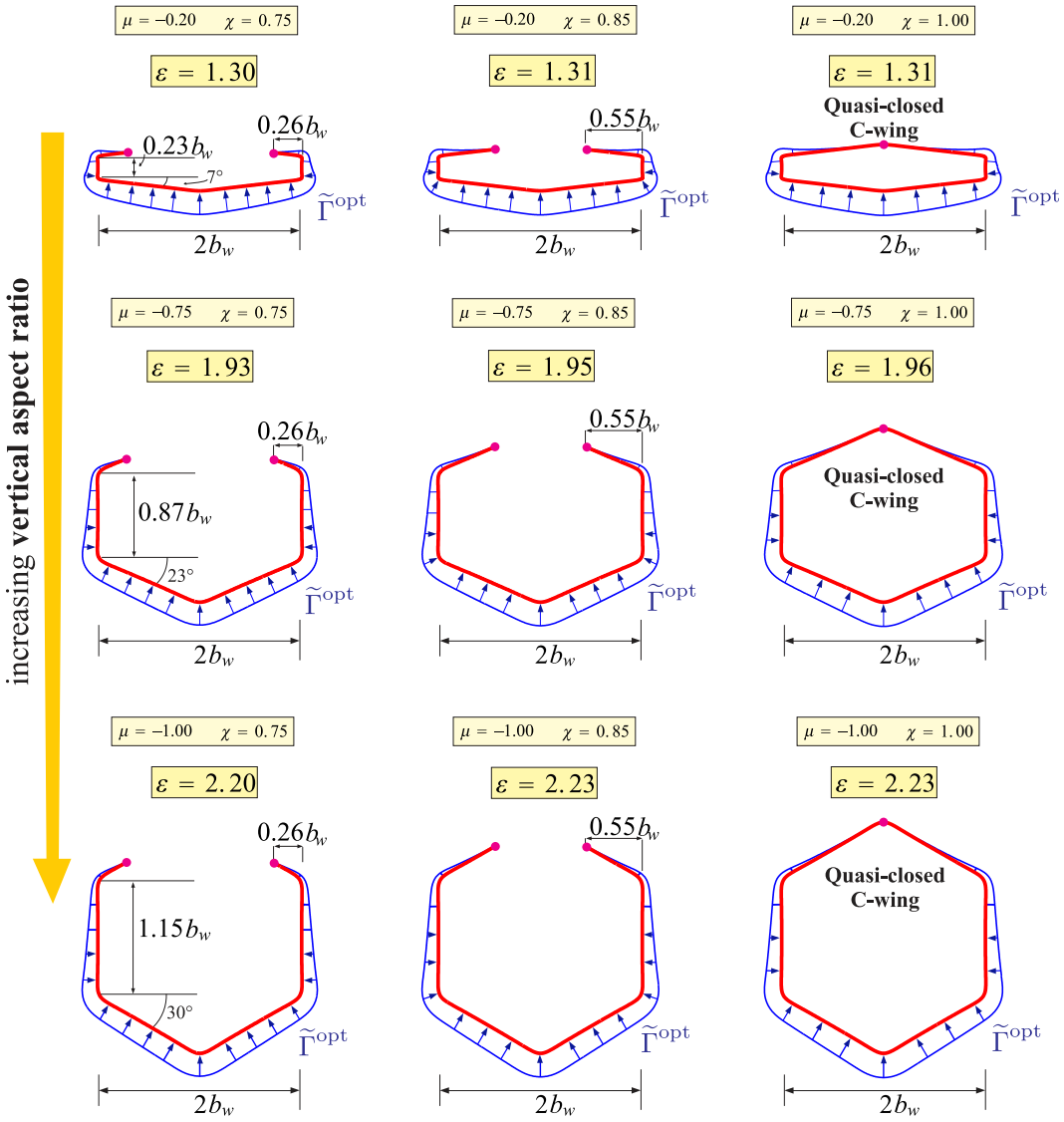

Figure 20. Optimal conditions for various highly non-planar wings. The superformula used to generate these cases is reported in equation 82

proportional to the cosine of the angle of inclination of the lifting element at that point. The constant of proportionality is the ratio between the freestream velocity and the optimal aerodynamic efficiency.

The general formulation can also be used to demonstrate induced drag theorems. In particular, the Minimum Induced Drag Curvature-Invariance Theorem (MIDCIT) and the Quasi-closed C-Wing Zero-gradient Optimal Circulation Theorem (QCWZOCT) are introduced, demonstrated and the implications on the minimum induced drag conditions for various wing systems are discussed.

An efficient numerical procedure for the minimization problem is also introduced. This could be used in the early stages of the design for a quick estimate of the optimal induced drag conditions. Within a few seconds on a common laptop, the present procedure (implemented in MATLAB) provides optimal circulation distributions, aerodynamic efficiency, and induced drag.

It is numerically verified that a quasi-closed C-wing presents the optimal induced drag of the corresponding closed system. Although a formal demonstration is not available yet, this confirms the claims in the literature.

Open questions still need an answer. Besides the demonstration of the conjecture that a quasi-closed C-wing presents the same optimal efficiency of the corresponding closed wing, it needs to be investigated the

issue of asymptotic behavior of the optimal induced drag of boxwings (see the discussion earlier presented in the introduction). Moreover, a formal proof of the Augmented Munk's Minimum Induced Drag Theorem for closed systems and multi-wings is not yet available. Future work will address these open questions and investigate the existence of additional induced drag theorems.

XVI. Appendix: A Useful Mathematical Identity

Under the assumption that has been made on the curve ℓ, i.e., on its parametrization $\boldsymbol{\psi}(u), u \in [-1,1]$, and on the circulation Γ^{opt}, it can be shown that the mathematical identity reported below, that have been used to derive some of the key results presented in this paper, holds.

Let $\delta(\eta)$ be a smooth function in $[-a,a]$ vanishing at the endpoints $-a,a$. Then, the following relation holds:

$$\int_{-a}^{a} \delta(\eta) \fint_{-a}^{a} \frac{\mathrm{d}\Gamma^{\mathrm{opt}}(\xi)}{\mathrm{d}\xi} Y(\eta,\xi)\ \mathrm{d}\xi\mathrm{d}\eta = \int_{-a}^{a} \Gamma^{\mathrm{opt}}(\eta) \fint_{-a}^{a} \delta'(\xi)\ Y(\eta,\xi)\ \mathrm{d}\xi\mathrm{d}\eta \tag{83}$$

To prove this relation, recalling (33) the left hand side of (83) is rewritten as follows:

$$\int_{-a}^{a} \delta(\eta) \fint_{-a}^{a} \frac{\mathrm{d}\Gamma^{\mathrm{opt}}(\xi)}{\mathrm{d}\xi} Y(\eta,\xi)\ \mathrm{d}\xi\mathrm{d}\eta = \int_{-a}^{a} \delta(\eta) \fint_{-a}^{a} \frac{\mathrm{d}\Gamma^{\mathrm{opt}}(\xi)}{\mathrm{d}\xi} \left(-\frac{\mathrm{d}}{\mathrm{d}\eta} \ln|\mathbf{r}(\xi)-\mathbf{r}(\eta)|\right)\ \mathrm{d}\xi\mathrm{d}\eta \tag{84}$$

Next, it is recalled (see, for example, Remark 1 in [52]), that the (inner) Cauchy principal value integral of the right hand side can be rewritten in the form:

$$\fint_{-a}^{a} \frac{\mathrm{d}\Gamma^{\mathrm{opt}}(\xi)}{\mathrm{d}\xi} \left(-\frac{\mathrm{d}}{\mathrm{d}\eta} \ln|\mathbf{r}(\xi)-\mathbf{r}(\eta)|\right)\ \mathrm{d}\xi = -\frac{\mathrm{d}}{\mathrm{d}\eta} \int_{-a}^{a} \frac{\mathrm{d}\Gamma^{\mathrm{opt}}(\xi)}{\mathrm{d}\xi} \ln|\mathbf{r}(\xi)-\mathbf{r}(\eta)|\ \mathrm{d}\xi$$

Integrating by parts the latter integral, and recalling that $\Gamma^{\mathrm{opt}}(-a) = \Gamma^{\mathrm{opt}}(a) = 0$, the following relationship

$$\fint_{-a}^{a} \frac{\mathrm{d}\Gamma^{\mathrm{opt}}(\xi)}{\mathrm{d}\xi} \left(-\frac{\mathrm{d}}{\mathrm{d}\eta} \ln|\mathbf{r}(\xi)-\mathbf{r}(\eta)|\right)\ \mathrm{d}\xi = \frac{\mathrm{d}}{\mathrm{d}\eta} \fint_{-a}^{a} \Gamma^{\mathrm{opt}}(\xi) \frac{\mathrm{d}}{\mathrm{d}\xi} \ln|\mathbf{r}(\xi)-\mathbf{r}(\eta)|\ \mathrm{d}\xi =: F'(\eta)$$

is further obtained. Thus, the left hand side of relation (83) takes the form:

$$\int_{-a}^{a} \delta(\eta) F'(\eta) \mathrm{d}\eta$$

Under the assumptions made on the function $\delta(\eta)$, and noticing that $F(\eta)$ has only a *log* singularity at the endpoints $\eta = -a, a$, the latter integral can be integrated by parts. This gives:

$$\int_{-a}^{a} \delta(\eta) F'(\eta) \mathrm{d}\eta = -\int_{-a}^{a} \delta'(\eta) F(\eta) \mathrm{d}\eta$$

that is,

$$\int_{-a}^{a} \delta(\eta) F'(\eta) \mathrm{d}\eta = \int_{-a}^{a} \delta'(\eta) \fint_{-a}^{a} \Gamma^{\mathrm{opt}}(\xi) \left[-\frac{\mathrm{d}}{\mathrm{d}\xi} \ln|\mathbf{r}(\xi)-\mathbf{r}(\eta)|\right]\ \mathrm{d}\xi\mathrm{d}\eta$$

Finally, taking advantage of the identity (see [53], p. 171):

$$\int_{-a}^{a} \mathrm{d}\xi \fint_{-a}^{a} \frac{\Phi(\eta,\xi)}{\xi-\eta} \mathrm{d}\eta = \int_{-a}^{a} \mathrm{d}\eta \fint_{-a}^{a} \frac{\Phi(\eta,\xi)}{\xi-\eta} \mathrm{d}\xi$$

where in the case under consideration the function $\Phi(\eta,\xi) := \delta'(\eta)\,\Gamma^{\rm opt}(\xi)\,Y(\xi,\eta)\,(\xi-\eta) = -\delta'(\eta)\,\Gamma^{\rm opt}(\xi)\,q(\xi,\eta)$ satisfies the smoothness assumptions required in [53], after exchanging η with ξ the wanted identity (83) is obtained.

Acknowledgement. The authors thanks the referees for their careful reading of the manuscript and valuable comments.

References

[1]Céron-Muñoz, H. D., Cosin, R., Coimbra, R. F. F., Correa, L. G. N., and Catalano, F. M., "Experimental Investigation of Wing-Tip Devices on the Reduction of Induced Drag," *Journal of Aircraft*, Vol. 50, No. 2, March-April 2013, pp. 441–449.

[2]Henderson, W. P. and Holmes, B. J., "Induced Drag: Historical Perspective," *Society of Automotive Engineers Paper 892341*, 1989.

[3]Kroo, I., "Drag Due to Lift: Concepts for Prediction and Reduction," *Annual Review Fluid Mechanics*, Vol. 33, 2001, pp. 587–617.

[4]Alley, N. R. and Phillips, W. F., "Minimizing Induced Drag with Spanwise Blowing Variation on a Circulation-Controlled Wing," *Journal of Aircraft*, Vol. 47, 2010, pp. 2164–2168.

[5]Phillips, W. F., Fugal, S. R., and Spall, R. E., "minimizing Induced Drag with Wing Twist, Computational-Fluid-Dynamics Validation," *Journal of Aircraft*, Vol. 43, 2006, pp. 437–444.

[6]Yamazaki, W., Matsushima, K., and Nakahashi, K., "Aerodynamic Design optimization Using the Drag-Decomposition Method," *AIAA Journal*, Vol. 46, 2008, pp. 1096–1106.

[7]Hicken, J. and Zingg, D. W., "Induced-Drag Minimization of Nonplanar Geometries Based on the Euler Equations," *AIAA Journal*, Vol. 48, 2010, pp. 2564–2575.

[8]Kravchenco, S. A., "The Application of the Wing Lifting Surfaces for Practical Aerodynamic," *Proceedings of the 20th Congress of the International Council of the Aeronautical Sciences, Sorrento, Italy*, 1996.

[9]Prandtl, L., "Induced Drag of Multiplanes," *National Advisory Committee for Aeronautics, Technical Note No. 182, From Technische Berichte, Volume III, No. 7*, 1924, pp. 309–315.

[10]Kroo, I., "Nonplanar Wing Concepts for Increased Aircraft Efficiency," *VKI lecture series on Innovative Configurations and Advanced Concepts for Future Civil Aircraft*, 2005.

[11]La Roche, U. and Palffy, S., "WING-GRID, a Novel Device for Reduction of Induced Drag on Wings," *Proceedings of the 20th Congress of the International Council of the Aeronautical Scinces, Sorrento, Italy*, 1996.

[12]La Roche, U.and Piening, M., Stengele, I., and Bitanx, B. T., "Development, Qualifications and Flight Testing of a WiWingg on a jetpowered testbed," *Proceedings ICAS 98, Melbourne, Australia*, 1996.

[13]Kolonay, R. M. and Eastep, F. E., "Optimal Scheduling of Control Surfaces on Flexible Wings to Reduce Induced Drag," *Journal of Aircraft*, Vol. 43, 2006, pp. 1655–1661.

[14]Raveh, D. E. and Levy, Y., "CFD-Based Aeroelastic Response of an Active Aeroelastic Wing," *48th AIAA SDM Conference, AIAA Paper 2004-1515*, 2004.

[15]Weisshaar, T. A. and Duke, D. K., "Induced Drag Reduction Using Aeroelastic Tailoring with Adaptive Control Surfaces," *Journal of Aircraft*, Vol. 43, 2006, pp. 157–164.

[16]Katz, J. and Plotkin, A., *Low-Speed Aerodynamics*, Cambridge University Press, 2nd ed., 2002.

[17]Kálman, T. P., Giesing, J. P., and Rodden, W. P., "Spanwise Distribution of Induced Drag in subsonic Flow by the Vortex lattice Method," *Journal of Aircraft*, Vol. 7, 1970, pp. 574–576.

[18]Carmichael, R. L. and Erickson, L. L., "PANAIR- A Higher Order Panel Code for Predicting Subsonic or Supersonic Linear Potential Flow About Arbitrary Configurations," *AIAA Paper 81-1255*, 1981.

[19]Smith, S. C. and Kroo, I., "Induced Drag Computations on Wings with Accurately Modeled Wakes," *Journal of Aircraft*, Vol. 34, 1997, pp. 253–255.

[20]Smith, S. C., "A Computational and Experimental Study of Nonlinear Aspects of Induced Drag," *NASA Technical Paper 3598*, 1996.

[21]Weissinger, J., "Über die Auftriebverteilung von Pfeilflügeln," *Forschungsbericht der Berliner Zentrale fur wissenschaftliches Berichtswesen, 1553, Berlin-Adlershof*, 1942.

[22]Weissinger, J., "The Lift Distribution of Swept-Back Wings," *NACA TM 1120*, 1947.

[23]Munk, M., "The minimum Induced Drag in Airfoils," *NACA, Report 121*, 1921.

[24]Prandtl, L., "On Wings with Minimum Induced Drag," *Zeitschrift Flugtechnik und Motorluftschiffahrt*, Vol. 24, 1933, pp. 305–306.

[25]Jones, R. T., "The Spanwise Distribution of Lift for Minimum Induced Drag of Wings Having a Given Lift and a Given Bending Moment," *NACA TN-2249*, 1950.

[26]Klein, A. and Viswanathan, S. P., "Approximate Solution for Minimum Induced Drag of Wings with Given Structural Weight," *Journal of Aicraft*, Vol. 12, 1974, pp. 124–126.

[27]Pate, D. J. and German, B. J., "Lift Distributions for Minimum Induced Drag with Generalized Bending Moment Constraints," *Journal of Aircraft*, In press.

[28]Letcher, J. S., "V-Wings and Diamond Ring-Wings of Minimum Induced Drag," *Journal of Aircraft*, Vol. 9, 1972, pp. 605–607.

[29]Cone, C. D., "The theory of induceded lift and minimum induced drag of nonplanar lifting systems," Tech. rep., NASA, 1962, R 139.

[30]DeYoung, J., "Induced Drag Ideal Efficiency Factor of Arbitrary Lateral-Vertical Wing Forms," *NASA Contractor Report 3357*, 1980.

[31]Von Karman, T. and Burgers, J. M., "General Aerodynamic Theory- Perfect Fluids," *Vol II of Aerodynamic Theory*, 1935, pp. 201–222, Editor in Chief Durand W. F.

[32]Frediani, A. and Montanari, G., "Best Wing System: An Exact Solution of the Prandtl's Problem," *Variational Analysis and Aerospace Engineering*, 2009, pp. 183–211, Springer Optimization and Its Applications 33, DOI 10.1007/978-0-387-95857-6-11.

[33]Frediani, A., Montanari, G., and Pappalardo, M., "Sul problema di Prandtl della minima resistenza indotta di un sistema portante," *AIDAA*, November 1999, pp. 267–278.

[34]Rizzo, E., *Optimization Methods Applied to the Preliminary Design of Innovative, Non Conventional Aircraft Configurations*, Edizioni ETS, 2009, ISBN 978-884672458-8.

[35]Demasi, L., Dipace, A., Monegato, G., and Cavallaro, R., "An Invariant Formulation for the Minimum Induced Drag Conditions of Non-planar Wing Systems," *AIAA Journal*, 2014, In press.

[36]Panaro, M. T., Frediani, A., Giannessi, F., and Rizzo, E., "Variational Approach to the Problem of the Minimum Induced Drag of Wings," *Variational Analysis and Aerospace Engineering*, 2009, pp. 313–342.

[37]Ashenberg, J. and Weihs, D., "Minimum Induced Drag of Wings with Curved Planform," *Journal of Aircraft*, Vol. 21, 1984, pp. 89–91.

[38]Demasi, L., "Induced Drag Minimization: A Variational Approach Using the Acceleration Potential," *Journal of Aircraft*, Vol. 43, june 2006, pp. 669–680.

[39]Demasi, L., "A Theoretical Investigation on the Conditions of Minimum Induced Drag of Closed Wing Systems and C-Wings," *Journal of Aircraft*, Vol. 44, 2007, pp. 81–99.

[40]Gelfand, I. M. and Fomin, S. V., *Calculus of Variations*, Prentice-Hall, Inc., 1963, Translated from the Russian by Silverman R. A.

[41]Lebedev, L. P. and Cloud, M. J., *The Calculus of Variations and Functional Analysis with Optimal Control and Applications in Mechanics*, World Scientific Publishing, 2003.

[42]Reddy, J. N., *Energy Principles and Variational Methods in Applied Mechanics*, John Wiley & Sons, Inc., 2002, ISBN: 978-0-471-17985-6.

[43]Bacciotti, A., *Teoria Matematica dei Controlli*, CELID Turin, Italy.

[44]Anderson, J. D., *Fundamental of aerodynamics*, McGraw-Hill, 2001.

[45]Prössdord, S. and Silbermann, B., *Numerical Analysis for Integral and Related Operator Equations*, Birkhäuser, 1991.

[46]Junghanns, P. and Silbermann, B., "Numerical analysis for one-dimensional Cauchy singular integral equations." *Journal of Computational and Applied Mathematics*, Vol. 125, 2000, pp. 395–421.

[47]Elliott, D., "Rates of convergence for the method of classical collocation for solving singular integral equations." *SIAM J. Numer. Anal.*, Vol. 21, 1984, pp. 136–421.

[48]Berthold, D., Hoppe, W., and Silbermann, B., "A fast algorithm for solving the generalized airfoil equation." *Journal of Computational and Applied Mathematics*, Vol. 43, 1992, pp. 185–219.

[49]Venturino, E., "The Galerkin method for singular integral equations revisited." *Journal of Computational and Applied Mathematics*, Vol. 40, 1992, pp. 91–103.

[50]Abramowitz, M. and Stegun, I., *Handbook of Mathematical Functions*, National Bureau of Standards,, 1964.

[51]Gielis, J., "A Generic Geometric Transformation that Unifies a Wide Range of Natural and Abstract Shapes," *American Journal of Botany*, Vol. 90, No. 3, 2003, pp. 333–338.

[52]Monegato, G., "Numerical evaluation of hyper-singular integrals," *Journal of Computational and Applied Mathematics*, Vol. 50, May 1994, pp. 9–31.

[53]Tricomi, F., "Integral Equations," *Pure and Applied Mathematics. Vol. V, Interscience Publishers, Inc.*, 1957, pp. 1–238.